EVALUATION OF SNOWMELT ESTIMATION TECHNIQUES FOR ENHANCED SPRING PEAK FLOW PREDICTION

EVALUATION OF SNOWMELT ESTIMATION TECHNIQUES FOR ENHANCED SPRING PEAK FLOW PREDICTION

BY JETAL AGNIHOTRI, B.Eng

A Thesis Submitted to the School of Graduate Studies

In Partial Fulfillment of the Requirements

for the Degree Master of Science

McMaster University MASTER OF SCIENCE (2018) Hamilton, Ontario

(EARTH AND ENVIRONMENTAL SCIENCES)

TITLE: Evaluation of Snowmelt Estimation Techniques for

                                    Enhanced Spring Peak Flow Prediction

AUHTOR: Jetal J. Agnihotri, B.Eng (Gujarat Technological

                                    University)

SUPERVISOR: Dr. Paulin Coulibaly

NUMBER OF PAGES: xi, 88

Abstract

In cold and snowy countries, water resources management and planning require accurate and reliable spring peak flow forecasts which call for adequate snowmelt estimation techniques. Thus, exploring the potential of snowmelt models to improve the spring peak flow prediction has been an active research area. Snow models vary in degree of complexity from simple empirical models to complex physically based models. Whereas majority of studies on snowmelt modeling have focused on comparing the performance of empirical snowmelt estimation techniques with physically based methods, very few studies have investigated empirical methods and conceptual models for hydrological applications. This study investigates the potential of a simple Degree-Day Method (DDM) to effectively and accurately predict peak flows compared to sophisticated SNOW-17 model at La-Grande River Basin (LGRB), Quebec and Upper Assiniboine river at Shellmouth Reservoir (UASR), Manitoba. Moreover, since hydrologic models highly rely on estimated parameter vectors to produce accurate streamflow simulations, accurate and efficient parameter optimization techniques are essential. The study also investigates the benefits of seasonal model calibration versus annual model calibration approach. The study is performed using two hydrological models, namely MAC-HBV (McMaster University Hydrologiska Byrans Vattenbalansavdelning) and SAC-SMA (Sacramento Soil Moisture Accounting) and their model combinations thereof.

Results indicate that the simple DDM performed consistently better at both study sites and showed significant improvement in prediction accuracy at UASR. Moreover, seasonal model calibration appears to be an effective and efficient alternative to annually calibrated model especially when extreme events are of particular interest. Furthermore, results suggest that SAC-SMA model outperformed MAC-HBV model, no matter what snowmelt computation method,

calibration approach or study basin is used. Conclusively, DDM and seasonal model optimization approach coupled with SAC-SMA hydrologic model appears to be a robust model combination for enhanced spring peak flow prediction. A significant advantage of aforementioned modeling approach for operational hydrology is that it demonstrates computational efficiency, ease of implementation and is less time-consuming.

Acknowledgements

I would like to extend my gratitude to many people for their support throughout my graduate study.

Firstly, I would like to thank my supervisor Dr. Paulin Coulibaly. I appreciate the opportunity provided by you to pursue the research study here in McMaster University. This thesis would not have been possible without the guidance, support, time and patience given by you. I have learnt a tremendous amount due to this opportunity given to me. I would also like to acknowledge the financial support provided through the NSERC FloodNet grant for this research.

I am extremely grateful to Dr. Tara Razavi for her help and constructive suggestions provided throughout the modeling process. My sincere thanks to Dr. Dominique Tapsoba (Hydro-Quebec) and Dr. Fisaha Unduche (Manitoba Infrastructure) for providing datasets required for the study. I am very thankful to all the members of Water Resources and Hydrologic Modeling Lab for always being available to willingly answer my questions and offering me help. The productive suggestions and discussions with you have inspired me to learn more during these two years. I would also like to take this opportunity to thank the professors and staff of the School of Geography and Earth Sciences who have provided essential support in various aspects.

Finally, I would like to extend a special thanks to my family and friends. I am extremely grateful to my husband Falak Sutariya for your love and support, my mother Nita Agnihotri and father Janardan Agnihotri for your great encouragement and support and my brother Pujan Agnihotri for showing me the ropes. Support from Rajendra and Kundan Sutariya is greatly appreciated.

Table of contents

List of Figures

List of Tables

List of Abbreviations

RMSE	Root Mean Squared Error
PFC	Peak Flow Criteria
NSE	Nash-Sutcliffe Efficiency
KGE	Kling Gupta Efficiency
NVE	Nash-Volume Error
MI	Model Improvement
PSO	Particle Swarm Optimization
VE	Volume Error
MAC-HBV	McMaster University Hydrologiska Byrans Vattenbalansavdelning
SAC-SMA	Sacramento Soil Moisture Accounting
DDM	Degree Day Method
TIM	Temperature Index Method
LGRB	La-Grande River Basin
UASR	Upper Assiniboine river at Shellmouth Reservoir
MD	MAC-HBV with DDM as snowmelt routine
SD	SAC-SMA with DDM as snowmelt routine
MS	MAC-HBV with SNOW-17 as snowmelt routine
SS	SAC-SMA with SNOW-17 as snowmelt routine
SWE	Snow Water Equivalent
PRMS	Precipitation-Runoff Modelling System
SWAT	Soil and Water Assessment Tool

EBM	Energy Budget Method
HEC	Hydrologic Engineering Centre
HEC-1-H	Hydrologic Engineering Center – Hybrid Model
SSARR-T	Streamflow Simulation and Reservoir Regulation system – TIM
SSARR-E	Streamflow Simulation and Reservoir Regulation system – EBM
SHE	Système Hydrologique Européen
HMETS	Hydrological Model of Ecole de Technologie Supérieure
HBV	Hydrologiska Byrans Vattenbalansavdelning
ETI	Enhanced-Temperature Index
SEB	Simplified Energy Balance
ESCIMO	Energy Balance Snow Cover Integrated MOdel
SNTHERM	Snow Thermal Model
SNAP	Snowmelt Numerical Analytical Package
SHAW	Simultaneous Heat and Water model
UEB	Utah Energy Balance
SNOBAL	Snow Energy and Mass Balance Model
SRM	Snowmelt Runoff Model
JIM	Jules Investigation Model
MRB	Mean Relative Bias
NWSRFS	National Weather Service River Forecast Centre
corr	Correlation
Std	Standard Deviation

Chapter 1 – Introduction

1.1 Background and Rationale

Accurate time- and site- specific spring flood forecasting is essential to water resources management and planning. Reliable spring flow predictions are needed by operators of hydropower reservoirs as well as water resources managers, and hold considerable economic value through enhanced operational decision making, efficient hydroelectric power generation, reduced downstream flood occurrences and better managed hydraulic structures to curtail environmental risks. Despite these advantages, reliable spring flow prediction remain a challenging task. A few techniques that can be adopted for improving the spring flow prediction accuracy include 1) enhancing meteorological forecast and hydrometric input data (i.e., different input forcings) (see Ahmed et al., 2015; Coulibaly, 2003); 2) improving optimization techniques (i.e., different approaches to obtain optimal model parameters) (see (Awol et al., 2018; Krauße et al., 2012); 3) using multi-models (i.e., use different models and inter-compare their performances) (Etchevers et al., 2004; Mahanama et al., 2011; Troin et al., 2015) and 4) Modifying complexity of physical processes governing the hydrologic model structure (e.g. snowmelt routing or other representative water balance component)(Debele et al., 2010; Etchevers et al., 2004; Krauße et al., 2012; Rango and Martinec, 1995; Troin et al., 2015). Our focus herein is to investigate and analyze approaches 2), 3) and particularly 4).

Since spring flood forecasts are concerned, spring snowmelt freshet is the major cause of floods in the snow-dominated watersheds (Ahmed et al., 2015; Pomeroy et al., 2005). This implies the need for adequate snowmelt computation methods (Debele et al., 2010; Essery, 2003; Valeo and Ho, 2004). To determine snowmelt, various computational methods have been proposed ranging from simple temperature index methods to complex and multi-layered energy budget models and

hybrids between these two methods (Debele et al., 2010; Essery et al., 2009; Raleigh and Lundquist, 2012; Valeo and Ho, 2004). Recent review of snowmelt estimation methods (see Bokhorst et al., 2016; Moghadas et al., 2016) and advances in the snow model intercomparison studies can be found in (Essery et al., 2013, 2009; Rutter et al., 2009; Bowling et al., 2003b). Snow models selected herein are temperature-index models as they require only precipitation and temperature data while energy budget approach requires excessive data inputs such as radiation, wind, humidity, that are not generally available at most mountainous sites. Furthermore, empirically based degree-day method demonstrates similar, and often better, performance than physically based energy balance models (Debele et al., 2010; Förster et al., 2014; Rango and Martinec, 1995; Troin et al., 2015; WMO, 1986). Despite the effectiveness, simplicity, applicability and accuracy of degree-day method, it is frequently suggested to replace the method with more complex promising approaches to improve accuracy of snowmelt estimates and subsequent reservoir inflow predictions (Debele et al., 2010; Hock, 2003; Kustas et al., 1994; Rango and Martinec, 1995). SNOW-17, a more sophisticated process-based model used operationally by NWS (National Weather Service) to produce snow accumulation and melt forecasts in snow-dominated catchments across the US is used herein to investigate its effectiveness against the popular degree-day method.

In operational snow hydrology, in addition to assessing the benefits of one snow model over another, a pertinent issue that remains is the model parameter optimization which is an inherent component of the hydrologic modeling system (Awol et al., 2018; Krauße et al., 2012). Robust model calibration process depends on selection of representative calibration data, appropriate objective functions and advanced optimization algorithm/procedure, of which identifying a representative data set is a crucial factor and forms the basis of optimization process(Krauße et

al., 2012). In most operational procedures, it is a common practice to calibrate model based on annual time series (annual models) by partitioning the data into 75% and 25% for model training and testing periods respectively. Since the annual models are calibrated to minimize the error between observed and simulated inflows throughout the year, it can be computationally inefficient, thus time consuming and unproductive, particularly if extreme hydrologic events are of primary interest. An alternative approach is to consider seasonal time series of interest (herein spring season) in which parameters are adjusted to match specifically the recorded seasonal flows that can lead to efficiency in terms of time, computational cost and accuracy. Given the advantages of using seasonal models, a particular interest of the study is to assess the effectiveness of seasonal models.

1.2 Research objectives

Inspired by the challenges mentioned above, specific objectives of this study include:

1. Investigate the potential of two popular snowmelt models, the simple degree-day method and the more complex SNOW-17 model to improve the spring peak flow prediction in snow-dominated watersheds.

2. Evaluate the potential of seasonal model calibration approaches to enhance flood prediction as compared to annual model calibration methods using advanced global optimization algorithm (PSO).

3. To assess the performance of hydrological models and identify appropriate model for improved spring flood prediction.

4. Subsequently, assess and identify the effective combination of methods leading to better peak flow prediction.

To achieve aforementioned objectives, two hydrologic models (MAC-HBV and SAC-SMA) are used in conjunction with two snowmelt estimation methods (DDM and SNOW-17 model) and two calibration approaches (seasonal and annual) leading to 8 model structures. These model combinations were implemented at two snow-dominated watersheds in Canada namely; La-Grande River Basin (LGRB) in the Province of Quebec and Upper Assiniboine river at Shellmouth Reservoir (UASR) in the Province of Manitoba.

1.3 Thesis structure

Premises of the study and research objectives are described in **Sections 1.1 and 1.2** respectively. A literature review, presented in **Section 1.4,** was conduct to summarize the snowmelt estimation methods and their merits and shortcomings in terms of application, data requirements, advances, and efficacy. Literature review led to the selection of potential models to be used in the study that can aid forecasters in operational decision making. Since the snowmelt models are employed herein, it is necessary to select the study site where spring flows are snowmelt driven. Details about the study area and data used here are provided in **Chapter 2**. Description of the identified snowmelt models, hydrological models and the methods adopted to obtain Pareto optimal sets are discussed in **Chapter 3**. Given that objective of the thesis is to inter-compare two snow models, calibration approaches and rainfall-runoff models in terms of their potential to capture spring flows, the selection of appropriate evaluation criteria is essential. The details about model performance assessment criteria are presented in **Chapter 3**. Results obtained from the model performance evaluation in Chapter 3 are summarized in **Chapter 4** and it is followed with discussion on possible reasons of better model performance or decline in model performance. Finally, **Chapter 5** details the conclusions and recommendations drawn from the research.

A **Journal paper** was completed on the research findings and submitted to the **Journal of Hydrology: Regional Studies**.

1.4 Literature Review

When the rainfall-runoff models are applied in cold and snowy regions, a snowmelt estimation module is added to the rainfall-runoff models to account for snow water equivalent of the snowpack and combined they are referred to as snowmelt-runoff models. From the hydrological forecasting perspective, evaluating runoff models is more relevant than assessing snow models alone. Snowmelt-runoff models used in hydrological applications can be broadly classified according to the extent of physical principles applied in the modelling process. Empirical models involve mathematical equations relating input and output time series but do not consider features and processes of the catchment. These models are often termed as observation oriented models or data driven models since they require extensive data for calibration. Conceptual models, on the other hand, considers physical processes occurring in the system but in simplified form i.e., consists number of interconnected reservoirs which represents recharge by rainfall, infiltration and percolation and is emptied by evapotranspiration and runoff. Physically-based models consider principles of physical processes utilizing physically derived relationships in modeling. Unlike empirical models, these models do not require extensive observed data but estimation of large number of parameters that describes the physical characteristics of the catchment for calibration. It should be noted here that empirical, conceptual and physically-based models have the degree of complexity in increasing order(Devia et al., 2015).

Based on the aforementioned categorization, snowmelt models such as temperature-index models, hybrid models and energy budget models can be generally classified as empirical, conceptual and physically-based models respectively. The temperature index method solely uses

air temperature to index the energy fluxes. Whereas the energy balance models determine the net incoming energy to calculate heat added to the snowpack that eventually leads to melting of the snowpack. A combination of the above two model approaches is termed as hybrid models. Owing to the varying complexity and nature of snow models, review of snowmelt estimation techniques is essential to determine the snowmelt estimation method that can be used in this study. The objectives of this review include: 1) To review the snowmelt estimation techniques according to the classification described previously 2) Summarizing the selected advances in snowmelt models reviewed in objective 1 3) Discuss the merits and limitations of snowmelt models in terms of ease of application, data requirements, accuracy and efficiency. Literature review presented herein does not emphasize on modeling urban snowmelt, since interest of this study is to model snowmelt particularly in undeveloped, forested and alpine sites. For recent review on urban snowmelt runoff modelling, interested reader is referred to (Moghadas et al., 2016). The following review will lead to determination of the method used in this research.

1.4.1 Temperature Index Models

Temperature index models (TIM) or degree-day method (DDM) has existed since its inception several decades ago. Although the origin of the TIM is difficult to attribute to one author, it could be traced back to (Finsterwalder and Schunk, 1887) who might have been the first to investigate relationship between air temperatures and melt rates for an alpine glacier. Other pioneers include (Horton, 1915) who tested melting of snow using experiments conducted in Albany, New York, USA to determine the rate of disappearance of a column of snow under constant temperature conditions. These preliminary tests concluded that each degree of temperature above 0°C was able to melt 0.04-0.06 inches of depth of SWE per day. (Clyde, 1931) conducted field experiments on snow melting in the mountains of Utah and concluded that

rainfall alone plays a minor role in snowmelt, but air temperature and melt are highly correlated. Additionally, it was also found that snowmelt degree-day was a constant and its value was estimated during experiments. Following which, (Collins, 1934) attempted to determine a relationship between degree-days above freezing and runoff to obtain predicted water supply for hydropower management using prediction curves in Spokane River, Idaho. In the light of estimating snowmelt-fed streamflow in remote locations of Sierra Nevada and due to time and meteorological data constraints, (Linsley, 1943) used degree-day method and concluded that degree-day number may be nearly constant. Since then, Degree-day method has been evolving and is widely applied in different hydrological applications to model snowmelt induced runoff (Cazorzi and Dalla, 1996; Debele et al., 2010; DeWalle et al., 2002; DeWalle and Rango, 2008; Hamlin et al., 1998; Hock, 1999, 2003; Hottelet et al., 1994; Kuusisto, 1980; Magnusson et al., 2015a; Martinec, 1960; Ohmura, 2001; Rango et al., 2008; Rango and Martinec, 1995; Speers, 1995; Troin et al., 2015; WMO, 1986). It considers temperature to be the major driving force of snowmelt processes. The underlying assumption behind the degree-day approach is that there is a linear relationship between snowmelt rates and average daily air temperature above some base temperature (DeWalle and Rango, 2008). The most basic formulation relates melt rate (M, mm) to the product of temperature differences between mean daily air temperature (T_a) and melt temperature(T_m, °c) (base temperature, usually 0°c) with degree-day factor (DDF, mm/day°C). Melt is expressed in terms of positive temperatures and its equation is given as follows:

$$M = (T_a - T_m) \times DDF \tag{1}$$

Snowmelt/snowmelt-runoff models that use different formulations of DDM are Hydrologiska Byråns Vattenbalansavdelning (HBV/HBV-light,(Bergstrom, 1976)), European Hydrologic System Model (MIKE-SHE,(Abbott et al., 1986)), Streamflow Simulation and Reservoir

Regulation System-Temperature index (SSARR-T,(Speers, 1995)), Hydrological Model of Ecole de Technologie Supérieure (HMETS,(Vehvilainen, 1992)), Snowmelt Runoff Model (SRM,(Martinec, 1975)), WINTER (Scheider et al., 1983)). Brief overviews of the selected Temperature Index Models are presented hereafter. HBV uses similar equation as (1) to compute snowmelt but snowpack is allowed to retain meltwater and when the observed air temperature declines below the threshold temperature, the liquid water within the snowpack refreezes based on the following equation:

$$RSWE_i = c_r \times cf_{max} \times (T_m - T_a) \tag{2}$$

Where, $RSWE_i$ is the amount of water that refreezes on day i (mm), c_r is the refreezing melt factor (mm/day°C).

HMETS model considers liquid water refreezing process, snowmelt and snowpack water retention capacity where snowmelt *(M)* on day *i* can be computed as below:

$$M = max(0, ddf_i(T_a - T_m)) \text{ when } T_a > T_m \tag{3}$$

Where, ddf_i is the degree-day factor that varies between minimum (ddf_{min}) and maximum value as a function of cumulative melt (CM_i, mm) and empirical parameter (k, mm^{-1}) given by equation (4), T_i and T_m are the mean daily temperature on day i and melt temperature respectively.

$$ddf_i = ddf_{min}(1 + k \times CM_i) \tag{4}$$

CM_i accounts for snowpack aging in the HMETS model.

SRM model computes snowmelt (*M)* based on following equation (Melloh, 1999):

$$M = ddf \times T_d \tag{5}$$

ddf is the degree-day factor (mm/°Cday) and T_d are degree-days(°Cday), mean daily temperature over 24 hrs or average of the minimum and maximum temperature over a day.

HEC-1 models snowmelt according to equation similar to (1) but snowmelt algorithm can also be switched to simplified energy balance approach (discussed below in hybrid models section). SSARR-T uses degree-day approach similar to HEC-1 model with the variation in degree-day melt coefficient which can be altered at a finer temporal resolution of a day(Melloh, 1999).

1.4.2 Hybrid Models

Hybrid models are referred to herein as the models which either use extended formulations of DDM or simplified variants of Energy Budget Methods (EBMs) to predict snowmelt. The latter method adds radiation component to the degree-day melt equation or uses empirical equations to compute energy fluxes(Hock, 2003). Hybrid models have gained popularity since they are better trade-offs between data-intensive, physically based EBMs and simplicity of DDM. Hybrid methods used to simulate snowmelt can be found in SNOW-17 model(Anderson, 2006, 1973), Snowmelt Runoff Model- Hybrid variant (SRM-H; (Kustas et al., 1994), Hydrologic Engineering Centre's Hybrid version(HEC-1-H;(USACE, 1998)), Enhanced-Temperature Index (ETI;(Pellicciotti et al., 2005)), HYDROTEL(Fortin et al., 2001), Simplified Energy Balance (SEB;(Chang and Fossum, 1997)). A brief description of the selected hybrid models is presented hereafter. SNOW-17 model uses DDM (equation 6) during non-rain periods to calculate melt (M_{nr}).

$$M_{nr} = M_f (T_a - T_m) \tag{6}$$

Where, M_f = seasonally varying melt factor, T_m = Melt temperature, T_a = Air temperature. During rain-on-snow periods, empirical energy balance equations are adapted considering several meteorological conditions in the SNOW-17 model. Detailed description on the SNOW-17 model is provided in **Section 3.2.2**. HYDROTEL considers processes such as air-snow and snow-ground interaction, snow compaction, albedo and liquid water retention capacity using partially empirical relationships to derive snowmelt. Melt is estimated in HYDROTEL by the following relationship:

$$M_i = \frac{-U_i}{C_f \times \rho_w} \tag{7}$$

Where, U_i is the calorific deficit on day i calculated by equation (8), C_f is the melting heat and ρ_w is the water density.

$$U_i = U_{i-1} + U_{n,i} + U_{p,i} - U_{c,i} - U_{a-s,i} - U_{g-s,i} \tag{8}$$

Here, $U_{n,i},\ U_{p,i},\ U_{c,i},\ U_{a-s,i},\ U_{g-s,i}$ denotes calorific deficit from solid precipitation, liquid precipitation, heat losses by convection, air-snow interface melt, snow-ground interface melt respectively on day i expressed in J/m^2 units. SRM model described in **Section 1.4.1** also falls in category of hybrid model when melt (M) is estimated using restricted degree-day radiation approach as follows (Melloh, 1999):

$$M = r \times T_d + m_Q \times R \tag{9}$$

Here, r = Constant restricted degree-day factor (cm/day°C);

m_Q = physical constant converting radiation to Snow Water Equivalent (SWE)

(0.026 cm.d^{-1}. (w/m^2)$^{-1}$)

R= net radiation (w/m^2)

Similarly, SEB considers empirical relationships to derive mass and energy balances of the snowpack as follows:

$$M = \frac{-Q_{s,i}}{\rho \times L_f} \times 1000 \tag{10}$$

Here, $Q_{s,i} = ISR_i \times (1 - a_i) + C_o + C_1 \times T_i$ (11)

$Q_{S,i}$ is the energy available for snowmelt on day i (W/m^2); ρ is the snow density (kg/m^3); Lf is the latent heat of fusion (J/kg); ISR_i the incoming shortwave radiation on day i (W/m^2); a_i is the time-varying snow albedo and $C0$ and $C1$ are two empirical factors accounting for the temperature-dependent energy fluxes (net longwave radiation and turbulent heat fluxes) (W/m^2 and W/m^2/°C, respectively).

Interestingly, SEB estimates the snow albedo as time dependent variable given by logarithmic function of accumulated maximum positive temperature since last snowfall:

$$a_i = p_1 - p_2 \log_{10} \times T_a \tag{12}$$

Where, Ta_i is accumulated daily maximum temperatures above 0 °C since snowfall on day i (°C); and $p1$ and $p2$ are empirical coefficients, where $p1$ is the albedo of fresh snow (for Ta = 1 °C).

HEC-1-H considers clear sky and cloudy conditions separately while estimating melt. During rain, cloudy weather conditions are presumed to prevail and melt (inch/day) can be calculated as:

$$M = C_1 \times [(0.029 + 0.0084kv + 0.007\,\text{Pr})(T_a - T_b) + 0.09] \tag{13}$$

Where k is basin convection-condensation constant (dimensionless), v =Mean wind speed at 50-ft height (miles/hr), P_r= Precipitation (inch/day), T_a= temperature saturated air at 10 ft (°F), T_b is

base melt temperature, C_1 is Coefficient of variation (dimensionless). When there is no rainfall, 50% forest canopy cover is assumed and melt is derived as follows:

$$M = C_2\left(k'(1-F)(0.004I_i)(1-\alpha) + k(0.008v)(0.22T_a') + k(0.008v)(0.78T_a') + F(0.029T_a')\right) \quad (14)$$

Here, k'= Shortwave radiation melt factor, F = Average basin forest canopy coverage, I_i= Solar radiation incident on a horizontal surface, T_a'= Air (10ft) and snow temperature difference, T_d'= Dew point and snow surface temperature difference, C_2= Coefficient of variation. Term 1 to 4 represents melt due to direct solar radiation, convection, condensation and longwave radiation respectively. Except the meteorological data inputs in equation (13 &14), other inputs are either considered constant or estimated through empirical relationships.

1.4.3 Energy Budget models

Energy Balance Models (EBMs) consider incoming, outgoing and stored energy in the system to determine the net incoming energy. If the net energy is positive, heat is added to the system that will lead to snowmelt. The rate at which snow will melt depends on the amount of energy added to the system (Debele et al., 2010). EBMs are applied in a wide range of snow, glacier and avalanche hydrology studies advocating its physical-basis(Abbott et al., 1986; Albert and Krajeski, 1998; Bathurst et al., 1995; Bathurst and Cooley, 1996; Bowling et al., 2003; Chang and Fossum, 1997; Essery et al., 2013; Etchevers et al., 2004; Förster et al., 2014; Georgievsky et al., 2007; Hock and Holmgren, 2005; Jordan, 1990; Koivusalo et al., 2001; Kumar et al., 2013; Magnusson et al., 2015a; Marks et al., 1999; Rutter et al., 2009; Strasser et al., 2002; Strasser and Marke, 2010; Tarboton and Luce, 1996; Todd et al., 2005). The most basic formulation of energy balance method can be depicted as follows(DeWalle and Rango, 2008):

$$\Delta Q_i = Q_{ns} + Q_{nl} + Q_h + Q_e + Q_r + Q_g + Q_m \quad (15)$$

Where, ΔQ_i = Change in internal snowpack energy storage ($\pm$)

Q_{ns} = net shortwave radiation energy exchange (≥ 0)

Q_{nl} = net longwave radiation energy exchange ($\pm$)

Q_h = convective exchange of sensible heat with the atmosphere ($\pm$)

Q_e = convective exchange of latent heat of vaporization and sublimation with the atmosphere ($\pm$)

Q_r = rainfall sensible and latent heat (≥ 0)

Q_g = ground heat conduction ($\pm$)

Q_m = loss of latent heat of fusion due to meltwater leaving the snowpack (≤ 0)

All the flux terms above are commonly expressed in J/sm^2 or W/m^2. In snowmelt estimation methods, Q_m is solved as a residual in equation (15), through which mass flux density of melt water (M) can be obtained.

$$M = \frac{Q_m}{\rho_w \times L_f \times B} \tag{16}$$

In which, ρ_w is the density of liquid water, L_f is latent heat of fusion and B is the thermal quality of snow. Models that employ EBMs to simulate snowmelt are Snow Thermal model (SNTHERM; (Jordan, 1990)), Energy Balance Snow Cover Integrated MOdel (ESCIMO;(Strasser et al., 2002)), Streamflow Simulation and Reservoir Regulation System-EBM (SSARR-E; (Speers, 1995)), Snowmelt Numerical Analytical Package (SNAP; (Albert and Krajeski, 1998), Soil and Water Assessment Tool (SWAT; (Neitsch et al., 2005)), Simultaneous Heat and Water model (SHAW; (Flerchinger, 2000)), Utah Energy Balance (UEB; (Tarboton and Luce, 1996), Snow Energy and mass Balance model (SNOBAL; (Marks et al., 1998)), SNOWPACK (Bartelt and Lehning, 2002), Precipitation-Runoff Modelling System (PRMS;(Markstrom, S. et al., 2015)). A brief summary of selected budget models is presented

hereafter. SNTHERM requires input variables such as air and dew point temperature, wind speed, precipitation and incoming values of solar and infrared radiation or cloud cover, solar aspect and inclination of surface. It considers processes such as snow accumulation, compaction, grain growth, melt, condensation melt, advection, pore water retention and melt flowing through the pack. Energy balance at the surface is given by:

$$Q_{sur} = Q_s \downarrow (1-\alpha_{sur}) + Q_l \downarrow - Q_l \uparrow + Q_{sen} + Q_{lat} + Q_p \tag{17}$$

The first term is incoming shortwave radiation, α is albedo, $Q_l \downarrow, Q_l \uparrow$ are the incoming and outgoing longwave radiation respectively, last three terms relate to sensible, turbulent and heat convection by precipitation respectively. SNAP model is unique in a way that it physically models flow of water through the snowpack, yet is computationally efficient (Melloh, 1999). Flow of water through the snowpack can be computed as follows:

$$\frac{\partial U}{\partial t} = n\phi^{-1}\left(1-S_{wi}\right)^{-1}\left[\frac{\rho_w kg}{\mu_w}\right]^{i/n} U^{1-\frac{1}{n}}\frac{\partial U}{\partial x} \tag{18}$$

Where, U is volume flux of water (cms^{-1}), t = time (s), n = dimensionless effective saturation exponent, ϕ=dimensionless porosity of snow, S_{wi} = irreducible water saturation of snow, ρ_w = density of water (g cm^{-3}), k = absolute permeability of snow (cm^2), g = acceleration due to gravity (cms^{-1}), μ_w = viscosity of water (gcm^{-1}s^{-1}) and x = vertical spatial coordinate (cm). SNAP computes the surface energy balance similar to equation (17) but it does not consider snow-soil energy exchange. PRMS models snowmelt in a two–layered system with heat conduction between the snow layers derived as:

$$Q_{COND} = 2\rho_s c_i \sqrt{\frac{K_E \Delta t}{\rho_s c_i \pi}} (T_s - T_p) \tag{19}$$

Here, ρ_s is snowpack density (g/cm^3), c_i is specific heat of ice (cal/g °C), K_s is effective snow thermal conductivity (cal/cm s °C) whereas T_s and T_p are snow surface temperature and temperature of the lower layer of snowpack. Energy balance at the snow-air interface (ΔQ) for the PRMS is computed for 12-hour durations (day and night) as:

$$\Delta Q = Q_{NS} + Q_{NL} + Q_{he} \tag{20}$$

Q_{NS} = Net shortwave radiation, Q_{NL} = Net longwave radiation, Q_{he} = Latent and sensible heat exchange. The soil-snow interface heat exchange is considered negligible while calculating snowmelt. UEB model updates the two variables; internal energy of the snowpack at top 40 cm of soil, U (kJ/m^2) and snow water equivalence, W (m) to compute melt rate according to equation (15) and (21) respectively:

$$\frac{dW}{dt} = P_r + P_s - M_r - S_r \tag{21}$$

Where, P_r is precipitation as rain, P_s is precipitation as snow, M_r is the melt rate and S_r is sublimation rate. UEB model requires the observations of precipitation, air temperature, humidity, wind speed and incoming solar radiation.

1.4.4 Merits and Limitations of Snow models

Snowmelt estimation methods categorized and described in the sub-sections 1.4.1, 2 & 3 have been successfully applied in a wide range of scientific studies. Selection of the snow model should depend on the factors such as modeling objectives, data availability, computational

constraints and spatial and temporal extent of application (DeWalle and Rango, 2008; Magnusson et al., 2015a). Based on the above criteria, in this subsection, the advantages and limitations of snow models will be addressed based on four major factors that have profound impact on model selection herein: 1) Data requirements 2) Accuracy 3) Computational efficiency and 4) Applicability.

Since DDM is an index model, it is not data intensive and requires only basic meteorological inputs of air temperature and precipitation for snowmelt prediction. In addition, relatively easy interpolation of air temperature data makes the implementation of DDM possible even for poorly gauged sites. This is a considerable advantage for operational hydrological applications such as flood forecasting and hydrologic modeling (Hock, 2003). Unlike DDM, hybrid models do not have fixed inputs, since data requirement for hybrid model is dependent on whether empirical relationships are used to simulate energy fluxes or radiation component is added to the simple DDM to finally compute snowmelt. For instance, SRM model (for details, see **Section 1.4.2**) uses restricted degree-day radiation approach and require the inputs of net radiation and SEB model needs the shortwave radiation observations to derive mass and energy balance through empirical relationships. However, SNOW-17 model, according to the previously mentioned categorization falls into hybrid model classification, but it only requires the observed precipitation and temperature data. Out of the 3 model categories, EBM is the most data intensive snowmelt estimation method as it not only needs precipitation and air temperature data but also requires radiation observations, wind speed, dew point temperature and humidity data. These data are generally not readily available at most sites due to which the application of EBM is restricted to limited operational use(Debele et al., 2010; Hock, 2003; Raleigh and Lundquist, 2012; Rango and Martinec, 1995; Troin et al., 2015). Therefore, implementation of TIM and

hybrid models is more common operationally. For instance, a review of operational snow models provided by (Melloh, 1999) mentioned that 3 TIMs and 2 hybrid snow models were used as operational snow models in US. Energy budget variants of the 2 operational models are also available, but these are implemented in case of availability of radiation observations.

Interestingly, despite having modest data requirements, DDM often performs comparable to or consistently better than complex physically based budget methods(Debele et al., 2010; Förster et al., 2014; Rango and Martinec, 1995; Troin et al., 2015; WMO, 1986). An international comparison of eleven snowmelt-runoff models conducted by (WMO, 1986) demonstrated the performance of DDM comparable to sophisticated energy budget formulations. Recently, (Debele et al., 2010) performed comparative analysis between the index models and energy budget methods in a physically based SWAT model at two watersheds in US and China. Their results suggest that TIM is better at predicting snowmelt induced runoff than budget models, when melt is governed by net solar radiation while sensible and turbulent heat fluxes have minimum effect. The ultimate reason of the success of DDM can be attributed to the high correlation between positive air temperatures and melt rates as well as temperature and several energy balance components(Hock, 2003). (Ohmura, 2001) analyzed the physical basis of TIMs and found that heat fluxes such as longwave radiation and sensible heat flux which contribute about 75% of the total heat for melt are highly affected by air temperature. Furthermore, since the single or multilayered budget method compute snowmelt based on physical laws, it involves complex physical process representations such as surface energy balance, heat flow through the snowpack, internal snowpack micro-structure that is explained by grain size, grain shape, bond size, sphericity and dendricity. Modeling these processes require high computational power. Whereas, the DDM and hybrid models estimate snowmelt through empirical relationships or

considering few physical processes but in simplified form which makes it computationally efficient. (Magnusson et al., 2015b) compared the performances of DDM with constant and variable degree-day factor, Jules Investigation Model (JIM) - a simplified version of EBM (belongs to hybrid model category) and SNOWPACK - a complex physically based layered snow model in the context of computational constraints, data availability and properties of interest. They revealed that the approximate runtime for the budget SNOWPACK model was 19000 times and 633 times higher than DDM and hybrid snow model respectively. This is a significant advantage for operational forecasters. Despite being time-consuming, their results indicate that higher model complexity does not translate to better model performance particularly for snowmelt estimation. This implies that DDM and hybrid models are as accurate as SNOWPACK model. However, the gradual need for evolution of snowmelt models from DDM to hybrid and energy balance methods is partially substantiated by the demand of higher temporal resolution simulations and prediction of the impacts of climate or land-use changes on large heterogeneous areas. In terms of temporal resolution, with an exception of (Hock, 1999), DDM models melt rates on a daily time step. (Hock, 1999) showed an application of DDM with sub-daily time steps by using diurnal variations in potential solar irradiation. In addition, the shift from DDM to EBM can also be attributed to represent the complex snow process in the snow models while considering the heterogeneous characteristics of the watershed in a spatially distributed manner. This does not mean that DDM cannot account for spatial variability; in fact, it was found to be accurate enough to account for complex snow processes by partitioning the watershed into elevation zones (Debele et al., 2010). Thus, although it is urged to use EBMs to quantify high temporal and spatial resolution melt, incorporating few processes in DDM can cater the demand. Whereas the application of EBMs is often limited to glacier and avalanche

hydrology and dynamics (Bartelt and Lehning, 2002; Brun et al., 1989; Troin et al., 2015), DDM has been applied to a wide range of snow hydrology studies as described earlier in **subsection 1.4.1**, particularly it has demonstrated better performance in large, forested and undeveloped watersheds(DeWalle and Rango, 2008; WMO, 1986). A considerable advantage of DDM is that it can be successfully applied when net radiation is the major driving force for snowmelt processes (applies for the sites used in this study) but not in maritime regions, where dominant sources of melt energy are sensible and latent heat fluxes (Debele et al., 2010).

Therefore, review of the advantages and limitations of the snow models based on the factors mentioned previously lead to the selection of DDM and hybrid model for snowmelt estimation. In the context of hybrid models, except HYDROTEL and SNOW-17 model, other snow models described in **sub-section 1.4.2** requires additional data i.e., most commonly radiation observations, which are typically unavailable at watersheds used in this study. Moreover, HYDROTEL model was originally developed to be compatible with remotely sensed and GIS data for distributed hydrologic modeling, not ground truth data. It consisted snow module as a component of the modeling system and was not specifically designed to model snowmelt. On the contrary, SNOW-17 model, widely used by National Weather Service River Forecast System (NWSRFS) for operational melt forecasting throughout the snow-dominated watersheds in US was specifically developed to estimate snowmelt. It has also been applied successfully in numerous snow hydrology studies and was one of the models evaluated by (WMO, 1986) in international comparison of snow models. Furthermore, (DeWalle and Rango, 2008) summarized the annual mean prediction statistics obtained by (WMO, 1986) which revealed that SNOW-17 model outperformed other snowmelt-runoff models when assessed at three watersheds. While the model only requires temperature and precipitation meteorological observed data, it is a

sophisticated hybrid model accounting for most of the important processes occurring in the column of snow in a simplified form. The model is described in further detail in **sub-section 3.2.2**.

Chapter 2 – Study Area and Data

The study was carried out at two watersheds in Canada namely; La-Grande River basin (LGRB), in the Province of Quebec and Upper Assiniboine river at Shellmouth Reservoir (UASR), in the Province of Manitoba to determine efficacy of the model structures in different hydrological regimes. Description of aforementioned study sites is provided below in section 2.1 and 2.2.

2.1 La-Grande River Basin (LGRB), Quebec

The LGRB lays in north-central Quebec (**Figure 1**) and contains the James Bay Hydroelectric Complex. Part of the Caniapiscau, Opinaca and Eastmain river flows were diverted to La-Grande River (Hernández-Henríquez et al., 2010). The present research includes La-Grande River and the diverted sub-watersheds, combined they are referred to as La-Grande River Basin (**Figure 1**). It spreads through the total drainage area of nearly 209,000 km^2 including the diverted basins and is primarily covered by forests (97%) and secondarily by water bodies (3%) (Coulibaly and Keum, 2016). According to the Canadian Climate Normals (1981-2010) at La-Grande River (53°38'N, 77°42'W), the mean annual precipitation is 697 mm out of which more than one-third is snowfall. Thus, peak runoff due to spring snowmelt is evident in the basin hydrology which is primary reason for basin selection. The average temperature ranges between -28°C to -8°C in winter (Jan-Mar) and -10°C to 17°C in spring (Apr-Jun). LGRB consists of 12 sub-catchments with each of its sub-basin containing a reservoir managed by Hydro-Quebec. The observed historical total precipitation, maximum and minimum temperatures and reservoir inflows were obtained on a daily time-scale for 36 years (1970-2005) from Hydro-Quebec. Different sub-basins comprised of varying data lengths. The 2 sub-basins that have more than 90% missing values were excluded from the study. Out of the 10 sub-watersheds left, 1, 2 and 7 number of sub-catchments consisted of 32 years, 22 years and 5 to 9 years of data lengths respectively. It is

worth noting that model was calibrated and validated for the precipitation, temperature and streamflow time series consisting of non-missing values to ensure proper training and testing of the models. Further sub-basin wise description of study area is given in **Appendix A**.
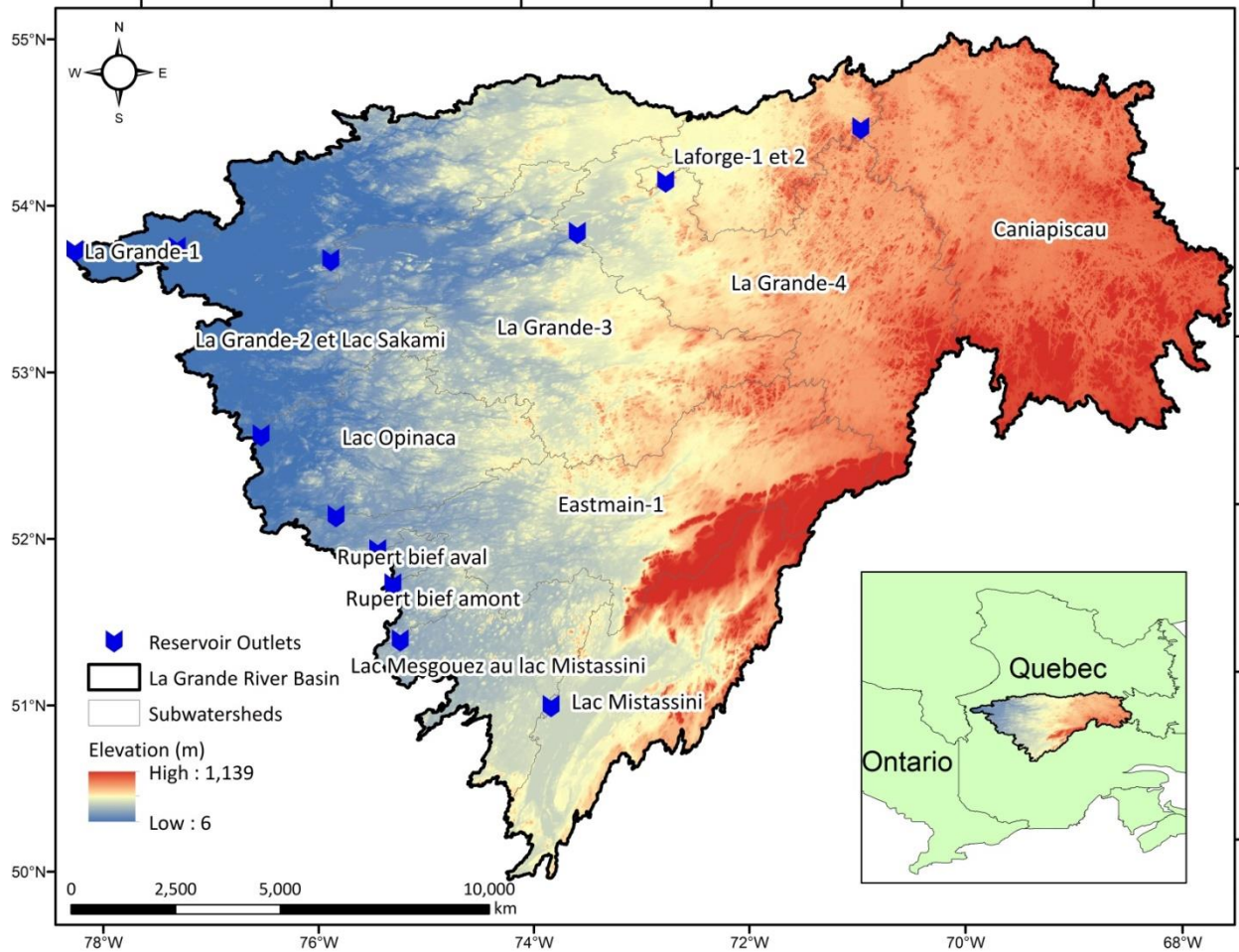
Figure 1: La-Grande River Basin (LGRB), Quebec

2.2 Upper Assiniboine river at Shellmouth Reservoir (UASR), Manitoba

The second study area is the Upper Assiniboine river at Shellmouth Reservoir which lays more than 80% in eastern Saskatchewan with remaining portion extending until Shellmouth Reservoir (Lake of the Prairies Reservoir) in western Manitoba with a gross drainage area of nearly 18,300 km^2 (**Figure 2**). It is to be noted that majority of this watershed lies in the prairie pothole region of the Canadian Prairies (Blais et al., 2016). For detailed understanding on the complex hydrology of the prairie pothole region, interested reader is referred to (Blais et al., 2016; Fang et al., 2007; Pomeroy et al., 2005). Based on 1981-2010 data, air temperature varies seasonally between -22°C to -1.4°C in winter (Jan-Mar) and -2.6°C to +21.8°C in spring (Apr-Jun), with about 511 mm of mean annual precipitation. UASR was selected for the experiment as it is a snow-dominated watershed with more than 80% of the total annual flow occurring during the spring snowmelt season (Fang et al., 2007; Shrestha et al., 2012). The observed daily precipitation, temperature, streamflow and reservoir inflow time series for the 23 years (1994-2015) period was provided by the Hydrologic Forecast Centre, Manitoba Infrastructure (MI). Calibration was conducted at Shellmouth reservoir inflow and at one of the major gauging stations feeding the reservoir, Assiniboine river at kamsack station. Station selection was based on factors such as least missing values and long records of data.
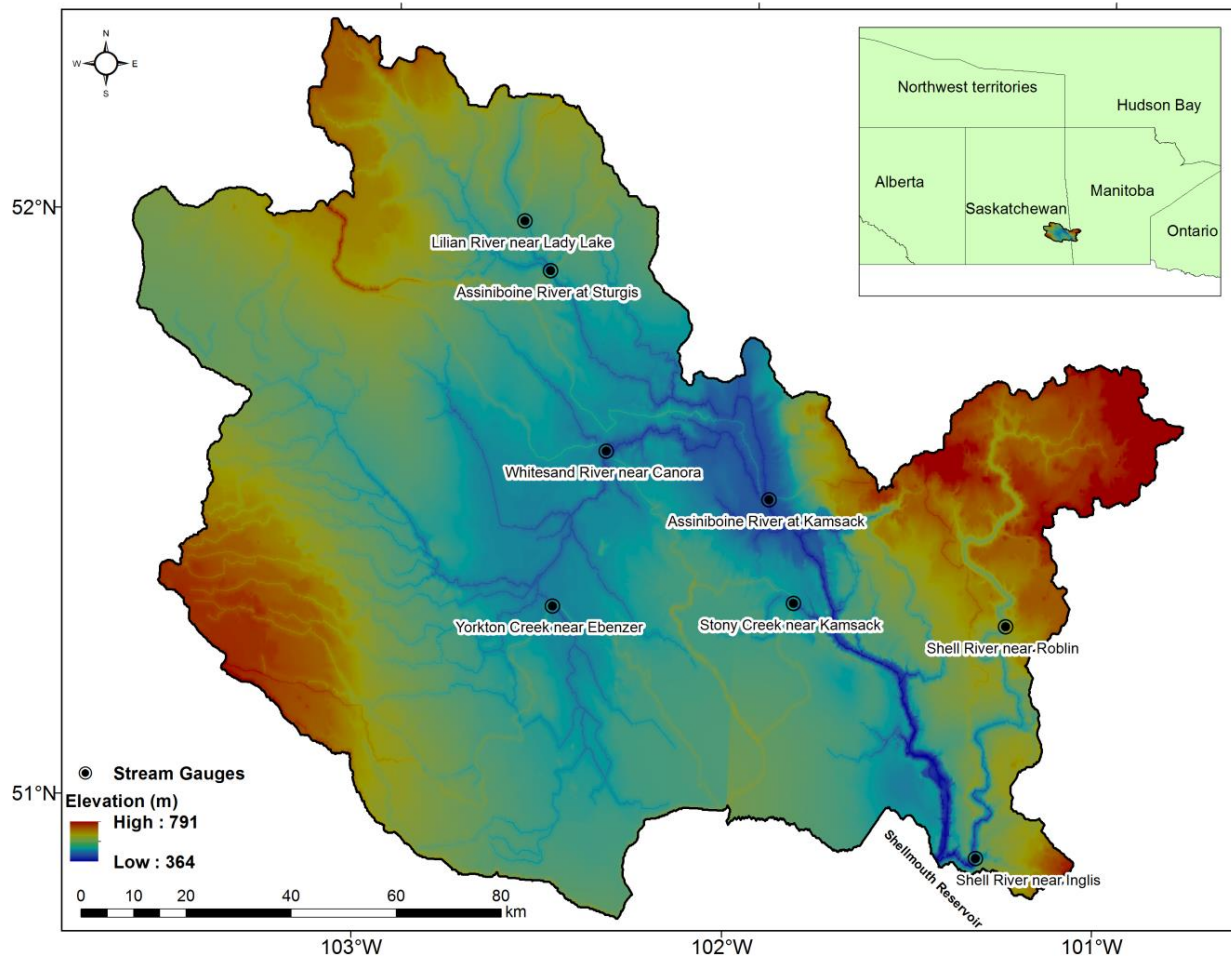
Figure 2: Upper Assiniboine river at Shellmouth Reservoir (UASR), Manitoba

Chapter 3 – Methodology

In this study, two hydrological models: MAC-HBV and SAC-SMA along with two snowmelt estimation techniques (Degree-day method and SNOW-17), and calibration approaches (annual and seasonal calibration) were investigated. Thus, four model structures namely; MAC-HBV DDM (MD), MAC-HBV SNOW-17 (MS), SAC-SMA DDM (SD) and SAC-SMA SNOW-17 (SS) with two scenarios i.e., annual and seasonal parameter optimization were examined for each model combination. Model set-up used herein is described in **Figure 3**. For annually and seasonally optimized models, the terms annual and seasonal models are used respectively. Each method is described in further detail in the following sub-sections.

3.1 Hydrological Models

3.1.1 MAC-HBV Model

The McMaster University Hydrologiska Byrans Vattenbalansavdelning (MAC-HBV) model, a lumped conceptual rainfall-runoff model developed by (Samuel et al., 2011) following the structure of HBV model (Bergstrom, 1976), has been successfully applied for wide range of hydrological studies (Razavi and Coulibaly, 2016; Samuel et al., 2012; Sharma et al., 2010, and others) including peak flow forecast studies(Ahmed et al., 2015). It comprises of snow routine, soil moisture routine, a response function and routing routine. The melt rate, obtained from the snowmelt estimation methods (see section 3.2), combined with precipitation as rain is provided to soil moisture routine. Changes in soil moisture storage of the top soil layer are represented by the soil moisture routine while daily potential evapotranspiration is determined by a simplified form of Thornthwaite equation. Runoff contribution from the upper and lower zone soil reservoir is represented by the response function after which equilateral triangular weighting function is

utilized for channel routing to obtain final streamflow. Detailed description of the model can be found in (Samuel et al., 2011).

The MAC-HBV model used herein is a semi-distributed variant of the model i.e., it was optimized at reservoir inflow of each sub-catchment for LGRB and at kamsack gauge station and reservoir inflow at UASR. The model requires daily precipitation and temperature time series as inputs to simulate daily flow. While the model adapted here is based on the daily scale, it is possible to reduce the temporal resolution of the model. The parameters calibrated herein, their description and ranges for the models used in the study are summarized in **Table 1**.

3.1.2 SAC-SMA Model

Sacramento Soil Moisture Accounting model (SAC-SMA)(Burnash et al., 1973) is a lumped conceptual watershed model operationally implemented by United States' National Weather Service River Forecast System (NWSRFS) for streamflow predictions and flood forecasts (Razavi and Coulibaly, 2016). It has been extensively used in previous studies in snowy regions (Day, 1985; Reed et al., 2004; Vrugt et al., 2006). SAC-SMA considers the precipitation to occur on pervious and impervious area and its accumulation in the upper and lower soil zone reservoirs as "tension" and "free" waters, if precipitation falls on pervious area or as direct runoff otherwise. The inputs to the model include daily precipitation and temperature time series, while it simulates the channel inflow, which is converted to streamflow using a simple Nash Cascade routing approach comprising of three linear reservoirs. The snowmelt component and evapotranspiration estimation used here is same as the MAC-HBV model. Although SAC-SMA is a lumped model, it was adapted in a semi-distributed manner calibrating at reservoir inflow of each sub-watershed for LGRB and at kamsack flow station and reservoir inflow for UASR.
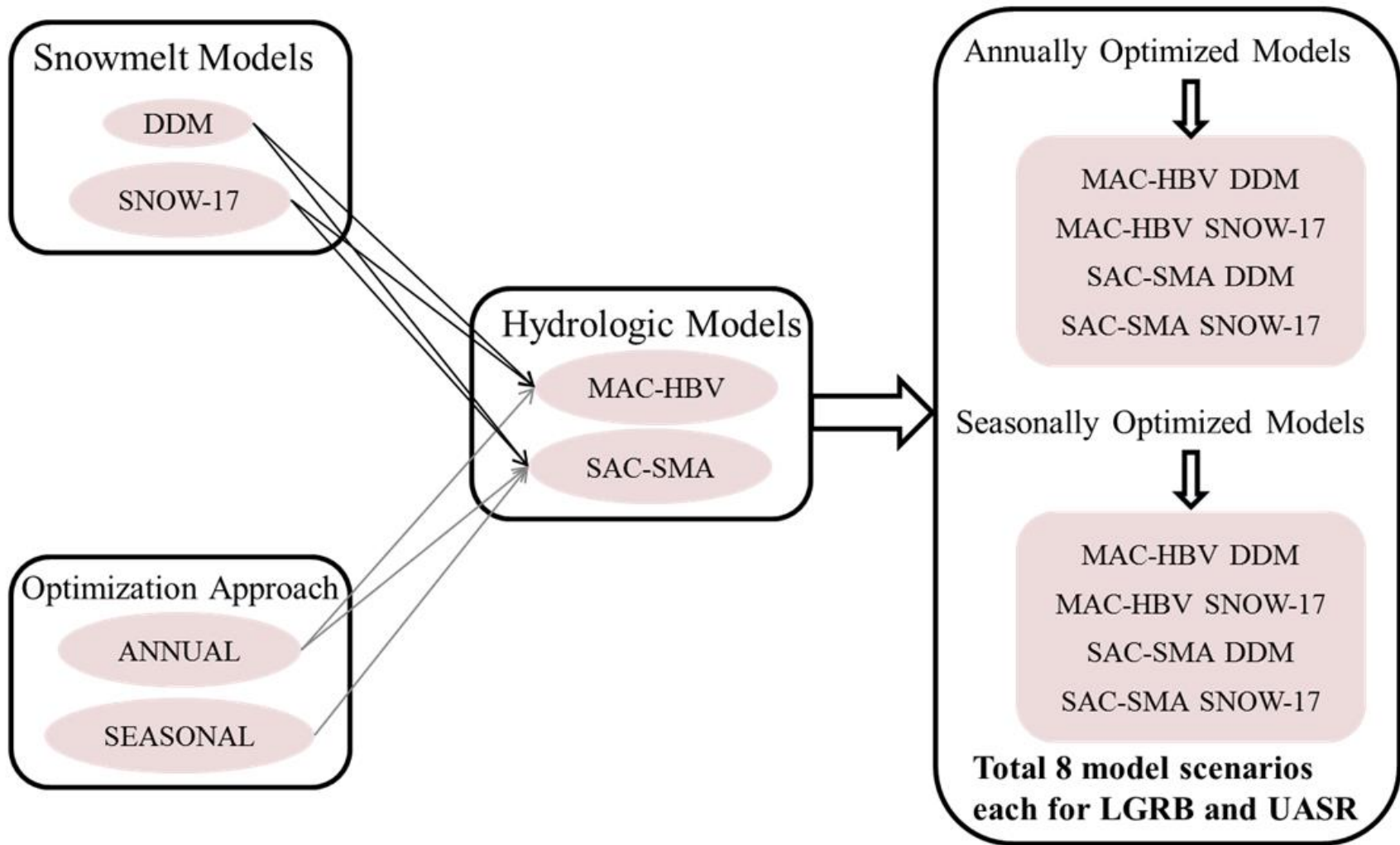
Figure 3: Model Set-up

3.2 Snowmelt estimation methods

3.2.1 Degree-day method

The degree-day method (DDM) is a temperature index approach relating to the widely used snow melt- air temperature relationship to obtain melt rate (Hock, 2003; Kustas et al., 1994; Ohmura, 2001). DDM has been evolving since its inception several decades ago(Förster et al., 2014; Hock, 2003; Rango and Martinec, 1995) varying in complexity from simple index models to extended versions that are referred to as simplified energy balance models (Hock, 2003). Extended DDM generally incorporates either radiation components in empirical form or considers seasonally variable degree day factors(Hock, 2003). Despite these complexities accounted in the snow model, extended formulations often perform similar to simple DDM (Debele et al., 2010; Hock, 2003; Troin et al., 2015). The variant of DDM used herein is similar to (Samuel et al., 2011). The melt rate (M) can be computed as the product of temperature differences between mean daily air temperature (T_a) and melt temperature(T_m) (usually 0°c) with degree-day factor (*DDF*). The melt equation is given by:

$$M = DDF(T_a - T_m), \quad \text{if } T_a > T_m \ \& \ \text{SWE>0} \tag{22}$$

$$M = 0, \text{ when } T_a < T_m \tag{23}$$

Here, changes in snow water equivalent (*SWE*) can be accounted as follows:

$$\Delta SWE = SCF(P_s - P_m) \tag{24}$$

Where, *SCF* is snow correction factor, P_s is snowfall (mm/day), P_m is meltwater (mm/day). Rainfall and snowfall amounts are determined by upper and lower threshold temperatures

distinguishing rain, snow and mix of snow and rain. Melt rate along with precipitation as rain is provided to hydrological model to obtain estimates of reservoir inflow.

3.2.2 SNOW-17 Model

SNOW-17 is a single-layer, process-based, temperature index model representing most of the complex physical processes occurring in the snow column (Anderson, 2006, 1973). The National Weather Service (NWS) produces operational snow accumulation and melt forecasts implementing SNOW-17 model for nationwide snow-dominated watersheds (Raleigh and Lundquist, 2012). Since the study sites are predominated by snowmelt and SNOW-17 model has demonstrated better prediction accuracy in some studies (Raleigh and Lundquist, 2012) and due to reasons mentioned in **sub-section 1.4.4**, it is used herein to compute snow melt. SNOW-17 considers processes such as energy exchange at the snow-air interface, heat storage and heat deficit of the snowpack, liquid water storage and transmission and also distinguish between rain-on-snow, rain-on-bare ground and non-rain events to model snow accumulation and ablation (Anderson, 2006). Despite being a sophisticated model, the inputs are daily precipitation and daily temperature which are readily available variables for most of the watersheds. It estimates outflow (snowmelt plus rain) and snow water equivalent (SWE), of which outflow is forcing to hydrologic models.

During rain-on-snow events, empirical energy balance equations are used to determine snowmelt utilizing several assumptions about meteorological conditions and is formulated as follows (Shamir and Georgakakos, 2006):

$$M_r = 3 \times 10^9 (T_a + 273)^4 - 20.4 + 0.0125 P T_a + 8.5 UADJ((0.9 e_s - 6.11) + 0.00057 P_a T_a) \qquad (25)$$

In which, T_a is air temperature, P is precipitation, P_a is atmospheric pressure, e_s is saturation vapor pressure. Here UADJ is the average wind function parameter that accounts for wind speed. It should be noted that melt computation during rain-on-snow events is independent of the time of the year. This implies that seasonal variations are not considered as the rate of snowmelt solely depends on observed precipitation and temperature.

Whereas, snowmelt during non-rain periods is varied seasonally since solar radiation can have profound effect during the melt season. Rate of snowmelt is expressed as:

$$M_{nr} = M_f (T_a - T_m) \tag{26}$$

Where, M_f is seasonally varying melt factor, T_m is melt temperature, T_a is air temperature. An important variable in equation 27 is the melt factor since incoming solar radiation as well as albedo of snow varies highly with the time of the year. To illustrate, albedo of the snow is higher in winter while it is lower for well-aged snow as the melt season progresses. Similarly, in the northern hemisphere, amount of maximum solar radiation is observed on June 21st while minimum solar radiation amount is around December 21st (Anderson, 2006). This implies the need for seasonal variation in the melt factor which is formulated as:

$$M_f = \Delta t_t / 6 \times [S_v A_v (MFMAX - MFMIN) + MFMIN] \tag{27}$$

Here, $MFMAX$= maximum melt factor on June 21st, $MFMIN$= minimum melt factor on December 21st, A_v= seasonal variation adjustment. A_v is dependent on the geographical coordinates and time of the year. Its value is highest when latitude is less than 54° and during the melt season i.e., April – August. S_v in equation 27 is updated as follows:

$$S_v = 0.5 \sin\left(\frac{(2N\pi)}{366}\right) + 0.5 \tag{28}$$

Where, N= number of day since March 21st

Table 1: Model parameters calibrated in the study with their descriptions, units and ranges

Parameter code	Description	Unit	Ranges
SAC-SMA			
UZTWM	Upper-zone tension water maximum storage	mm	1-150
UZFWM	Upper-zone free water maximum storage	mm	1-150
UZK	Upper-zone free water lateral depletion rate	day^{-1}	0.1-0.5
PCTIM	Impervious fraction of the watershed area	-	0-0.1
ADIMP	Additional impervious area	-	0-0.4
ZPERC	Maximum percolation rate	-	1-250
REXP	Exponent of the percolation equation	-	1-5
LZTWM	Lower-zone tension water maximum storage	mm	1-500
LZFSM	Lower-zone free water supplemental maximum storage	mm	1-1000
LZFPM	Lower-zone free water primary maximum storage	mm	1-1000
LZSK	Lower-zone supplemental free water lateral depletion rate	day^{-1}	0.01-0.25
LZPK	Lower-zone primary free water lateral depletion rate	day^{-1}	0.0001-0.025
PFREE	Fraction percolating from upper to lower zone free water storage	-	0-0.6
Rq	Routing coefficient	-	0.5-1.5
MAC-HBV			
athorn	Constant for Thornthwaite's equation	-	0.1-0.3
fc	Maximum soil box water content	mm	50-800

lp	Limit for potential evaporation	mm/mm	0.1*fc-0.9*fc
beta	Non-linear parameter controlling runoff generation	-	0-10
k0	Flow recession coefficient in an upper soil reservoir	days	1-30
lsuz	A threshold value used to control response routing on an upper soil reservoir	mm	1-100
k1	Flow recession coefficient in an upper soil reservoir	days	30-100
cperc	A constant percolation rate parameter	mm/day	0.01-6
k2	Flow recession coefficient in a lower soil reservoir	days	100-500
alpha1	An exponent in relation between outflow and storage representing non-linearity of storage – discharge relationship of lower reservoir	-	0.5-1.25
maxbas	A triangle weighting function for modelling a channel routing routine	days	1-20
DDM			
tr	Upper threshold temperature to distinguish between rainfall and snowfall	°C	0-2.5
scf	Snowfall correction factor	-	0.4-1.6
ddf	Degree day factor	mm/day°C	0-5.0
rcr	Rainfall correction factor	-	0.5-1.5
SNOW17			
scf	Snowfall correction factor	-	0.7-1.6
uadj	Average wind function during rain-on-snow events	mm/mb/6 h	0.03-0.19
mbase	Base temperature for non-rain melt factor	°C	0-1.0
mfmax	Maximum melt factor considered to occur on June 21	mm/6 h/°C	0.5-2.0

mfmin	Minimum melt factor considered to occur on December 21	mm/6 h/°C	0.05-0.49
tipm	Antecedent snow temperature index	-	0.01-1.0
nmf	Maximum negative melt factor	mm/6 h/°C	0.05-0.50
plwhc	Percent liquid-water holding capacity	-	0.02-0.3
pxtemp1	Lower limit temperature dividing transition from snow	°C	-2-0
pxtemp2	Upper limit temperature dividing rain from transition	°C	1-3

3.3 Model Optimization

The optimization was performed to obtain single set of best parameters that reproduces minimum error between observed and simulated streamflow. The four model combinations (MS, MD, SS, SD models) were calibrated for the even years considering the first year as spin-up and validated against the odd years provided the observed precipitation, temperature and streamflow data consisted of non-missing values. Annual as well as seasonal time series were optimized against the observed daily streamflow for the four model combinations. For the seasonal model training, spring months from March to July were considered in order to capture the rising and falling limb of the hydrograph. Recall that seasonal model experiment was carried out to test the ability of seasonal models to provide reasonably better agreement between observed and computed flows for the spring season. Particle Swarm Optimization algorithm (PSO, Eberhart and Kennedy, 1995) demonstrated superior performance in obtaining Pareto optimal set for hydrological models MAC-HBV and SAC-SMA specifically in terms of reducing volume error of peak flows in Canadian watersheds (Razavi and Coulibaly, 2017). Thus, PSO, a single objective, automatic

global optimization algorithm was selected herein to maximize the objective function NVE (Combined Nash-Sutcliffe efficiency and Volume error) after (Samuel et al., 2012) given by:

$$NVE = 0.5 NSE - 0.1 VE + 0.25 NSE_{Log} + 0.25 NSE_{Sqr} \tag{29}$$

Where Nash-Sutcliffe Efficiency (NSE) is defined as follows:

$$NSE = 1 - \left(\frac{\sum_{i=1}^{N} (Q_{obs} - Q_{sim})^2}{\sum_{i=1}^{N} (Qobs - \overline{Q_{obs}})^2} \right) \tag{30}$$

And Volume Error (VE) is formulated as:

$$VE = \frac{\sum_{i=1}^{N} Q_{sim} - \sum_{i=1}^{N} Q_{obs}}{\sum_{i=1}^{N} Q_{obs}} \tag{31}$$

The logarithm and square of NSE values can be expressed as:

$$NSE_{log} = 1 - \left(\frac{\sum_{i=1}^{N} (Log\ Q_{obs} - Log\ Q_{sim})^2}{\sum_{i=1}^{N} (Log\ Qobs - Log\ \overline{Q_{obs}})^2} \right) \tag{32}$$

$$NSE_{sqr} = 1 - \left(\frac{\sum_{i=1}^{N} (Q_{obs}^2 - Q_{sim}^2)^2}{\sum_{i=1}^{N} (Q_{obs}^2 - \overline{Q_{obs}^2})^2} \right) \tag{33}$$

Where *Qobs* and *Qsim* are the observed and simulated streamflow values, respectively, $\overline{Q_{obs}}$ is the average of observed streamflow values and *N* is the total number of data points. It is worth noting that Eqs. (32) and (33) are similar to Eq. (30) but accounting for log-transformed flows and square-transformed flows emphasizing on low flows and high flows respectively. NSE spans between -∞ to 1 with 1 showing optimal performance for NSE and NVE. Inversely, VE ranges from 0 to ∞ and values closer to zero reveals better model performance. Using equation (29), a single objective calibration approach can be used as a multi-objective approach. We revisited the objective function NVE (Equation (29)) to put more emphasis on high flows (NSE$_{sqr}$). The calibration was repeated for few model combinations with least performing sub-watersheds to check for improvement in performance, but we found that results did not improve peak flow statistics and hydrograph significantly. For the results of hydrographs showing the performance of NVE and modified NVE (more weight to high flows), refer to **Appendix B**. Henceforth, we include results obtained by training the models with above objective function eq. (29).

3.4 Model Performance Criteria

Given that the focus herein is to assess improvement in spring peak flows, the model performance was evaluated for the spring season i.e., April, May and June months for the 8 model structures during the entire period of study. To facilitate the assessment of snowmelt estimation techniques, model improvement (in percentage) in terms of percent reduction in the root mean squared error (RMSE, Eq. 34) when SNOW-17 model was adapted as compared to Degree-day method (taken as base model for evaluation), was used.

$$RMSE = \sqrt{\frac{1}{N}\sum_{i=1}^{N}(Q_{sim}-Q_{obs})^2} \qquad (34)$$

RMSE criterion was used to indicate the accuracy of the snowmelt estimation approaches and it is closer to zero for a perfect model. Positive values of model improvement indicate better performance of SNOW-17 model while negative values reveal model improvement due to implementation of DDM. The evaluation of annually and seasonally calibrated model as well as the two hydrologic models was carried out for the spring season and spring peak flow. Two criteria, namely NSE (Eq. 30) and Kling-Gupta Efficiency (KGE, (Gupta et al., 2009) (Eq.35)) were used to assess the spring season model performance.

$$KGE = 1 - \sqrt{(r-1)^2 + (a-1)^2 + (b-1)^2} \tag{35}$$

Where, $r = corr(Qsim, Qobs)$; $a = std(Qsim) / std(Qobs)$; $b = mean(Qsim) / mean(Qobs)$

KGE closer to unity is considered optimal. To test the ability of the models to capture spring peak flow, generally a threshold is selected based on peak over threshold, flow duration percentile or long-term median flow. In this study, we consider 75 percentile threshold and the flows above this threshold to be high flows. This threshold was selected to have similar number of peak flows for all the sub-watersheds and still have a reasonable number of days to calculate error. RMSE and Peak Flow Criteria (PFC) were selected to evaluate spring peak flow performance and were computed for flows over 75 percentile threshold. PFC can be calculated as follows (Coulibaly et al., 2001):

$$PFC = \frac{\left[\sum_{i=1}^{np} \left(Q_{obs} - Q_{sim} \right)^2 Q^2_{obs} \right]^{\frac{1}{4}}}{\left(\sum_{i=1}^{np} Q^2_{obs} \right)^{\frac{1}{2}}} \tag{36}$$

Where, n_p is the number of peak flows greater than 75 percentile, Q_{obs} and Q_{sim} are the observed and simulated flows respectively. PFC is considered a better performance indicator of prediction accuracy for the flood period and its value equal to zero represents optimal model performance.

The model performance evaluation criteria discussed above were computed using normalized streamflow to the area of each sub-watershed to be able to compare the sub-catchments with varying sizes.

Chapter 4 – Results and Discussion

In this chapter, performance of 8 model configurations and discussion on the results obtained is presented. Detailed description of the models, optimization process and evaluation criteria were reported in **Chapter 3**. First, the detailed findings obtained from evaluating the snowmelt estimation techniques used in the study are reported. Then, comparison of annually and seasonally calibrated models is presented to address objective 3. Further, hydrological models are analyzed to explore the approach that provides better estimates of spring peak flow and spring season. Lastly, visual inspection of hydrologic model configurations implemented herein is described. **Section 4.2** elaborates the findings discussed in results section by providing a critical analysis on outcome of the study.

4.1 Results

4.1.1 Evaluation of Snowmelt Estimation Methods: DDM and SNOW-17 model

Model improvement of training and testing periods when SNOW-17 model was used for the LGRB is presented in **Figure 4**. For both the MAC-HBV and SAC-SMA annually optimized models during the calibration period, the median is zero percent indicating the use of SNOW-17 model does not show any model improvement. In case of seasonally optimized models, median of MAC-HBV model reveals improvement of about 8% while SAC-SMA model median does not show any model improvement. For the validation period, implementing DDM improves the performance when coupled with MAC-HBV model whereas using SNOW-17 model improves the performance when used in conjunction with SAC-SMA model (Fig. 3). For instance, model median improved by about 4% when DDM is used with MAC-HBV model combinations, whereas the medians of model improvement with SAC-SMA annually and seasonally optimized models are ~7% and ~4% respectively with SNOW-17 model. However, difference between the

model performances of SNOW-17 and DDM snowmelt routines is relatively small suggesting that DDM has ability to perform comparable to SNOW-17 model. The model improvement for UASR presented in **Figure 5** depicts that using SNOW-17 model improves the performance when coupled with seasonal MAC-HBV model and SAC-SMA annual and seasonal models during the calibration period. The model improvement varies between 2% and 16%. However, whatever optimization approach or hydrologic model is used, the DDM significantly outperforms the SNOW-17 model during the model verification period. For example, median of model improvement varies between ~5% to ~36% when using DDM for all model combinations. In general, for the entire study period, median of 10 (out of 16) model scenarios show either model deterioration or no improvement due to the implementation of SNOW-17 model indicating DDM to be outperforming for most model combinations at both the study areas.

Spring peak flow statistics (Peak Flow Criteria (PFC)) (**Table 2 and 3**) at LGRB suggests that DDM and SNOW-17 model mean performs equally better in capturing the peak flow. It implies that 4 model combinations perform better with each snowmelt method. Furthermore, gaining insights into the sub-basin scale PFC statistics (**Table 6**) reveal that more than 55% of sub-basins perform better with DDM method at LGRB. Similarly, **Table 6** suggests that DDM is better at estimating peak flows for more than 60% of the sub-watersheds at UASR. Further investigation of NSE criterion at LGRB revealed that DDM was as accurate as SNOW-17 model (**Figure 6**) with relatively small differences in their model medians. While, during validation period, performance of MAC-HBV and SAC-SMA model combinations at UASR (**Figure 7**) indicated marked increase in median of NSE when DDM is used as compared to SNOW-17 model. Overall, DDM performed consistently better than SNOW-17 model evaluated for the spring season and spring peak flows at both watersheds and it outperformed significantly at UASR.

Table 2: Annual model performance statistics for LGRB

<div align="center">Annually Calibrated Model Performance Statistics -LGRB</div>

	Model Calibration Mean					Model Validation Mean				
Models	**NSE**	**KGE**	**NRMSE (mm/d)**	**PFC**	**Model Improvement (%)**	**NSE**	**KGE**	**NRMSE (mm/d)**	**PFC**	**Model Improvement (%)**
MAC DDM	0.76	0.83	1.49	0.40		0.56	0.68	1.83	0.46	
					1.13					-4.21
MAC SNOW-17	0.75	0.84	1.37	0.40		0.53	0.65	1.85	0.45	
SAC DDM	0.82	0.87	1.24	0.35		0.66	0.72	1.54	0.42	
					0.83					4.27
SAC SNOW-17	0.82	0.88	1.20	0.37		0.70	0.77	1.45	0.39	

Table 3: Seasonal model performance statistics for LGRB

<div align="center">Seasonally Calibrated Model Performance Statistics- LGRB</div>

	Model Calibration Mean					Model Validation Mean				
Models	**NSE**	**KGE**	**NRMSE (mm/d)**	**PFC**	**Model Improvement (%)**	**NSE**	**KGE**	**NRMSE (mm/d)**	**PFC**	**Model Improvement (%)**
MAC DDM	0.75	0.83	1.45	0.39		0.58	0.65	1.80	0.42	
					6.10					1.76
MAC SNOW-17	0.78	0.85	1.28	0.35		0.55	0.66	1.78	0.45	
SAC DDM	0.82	0.85	1.25	0.35		0.66	0.71	1.60	0.42	
					1.71					2.90
SAC SNOW-17	0.82	0.87	1.19	0.32		0.66	0.75	1.54	0.43	

Table 4: Annual model performance statistics for UASR

Annually Calibrated Model Performance Statistics -UASR

	Calibration					Validation				
Models	NSE	KGE	NRMSE (mm/d)	PFC	Model Improvement (%)	NSE	KGE	NRMSE (mm/d)	PFC	Model Improvement (%)
MAC DDM	0.48	0.74	0.32	0.47	3.07	0.56	0.57	0.54	0.53	-39.17
MAC SNOW-17	0.51	0.73	0.34	0.48		0.19	0.23	0.79	0.62	
SAC DDM	0.7	0.82	0.28	0.43	-4.14	0.49	0.52	0.59	0.57	-4.89
SAC SNOW-17	0.67	0.80	0.22	0.38		0.44	0.49	0.63	0.6	

Table 5: Seasonal model performance statistics for UASR

Seasonally Calibrated Model Performance Statistics- UASR

	Calibration					Validation				
Models	NSE	KGE	NRMSE (mm/d)	PFC	Model Improvement (%)	NSE	KGE	NRMSE (mm/d)	PFC	Model Improvement (%)
MAC DDM	0.42	0.72	0.36	0.49	17.67	0.52	0.6	0.54	0.52	-22.28
MAC SNOW-17	0.61	0.78	0.31	0.45		0.28	0.35	0.72	0.61	
SAC DDM	0.66	0.73	0.28	0.44	2.44	0.58	0.5	0.55	0.55	-13.20
SAC SNOW-17	0.68	0.73	0.28	0.46		0.46	0.48	0.65	0.59	

Table 6: Percentage of sub-basins performing better/competitive with a) DDM than SNOW-17 b) Seasonal than Annual model calibration and c) SAC-SMA than MAC-HBV model

|	Percentage of sub basins performing better/comparable with DDM than SNOW-17 model			Percentage of sub basins performing better/comparable with SEASONAL models than ANNUAL models				Percentage of sub basins performing better/comparable with SAC-SMA than MAC-HBV hydrologic model			
LGRB	**NSE**	**PFC**	**MI**	**NSE**	**KGE**	**PFC**	**NRMSE**	**NSE**	**KGE**	**PFC**	**NRMSE**
Entire Study Period	**51.25**	**56.25**	46.25	**53.75**	**51.25**	**51.25**	**53.75**	**92.5**	**78.75**	**73.75**	**86.25**
UASR	**NSE**	**PFC**	**MI**	**NSE**	**KGE**	**PFC**	**NRMSE**	**NSE**	**KGE**	**PFC**	**NRMSE**
Entire Study Period	**56.25**	**62.5**	**56.25**	**62.5**	38	**62.5**	**75**	**93.75**	**68.75**	**75**	**87.5**
Sum (LGRB+ UASR)	**52.1**	**57.3**	48	**55.2**	49	**53.1**	**57.3**	**92.7**	**77.1**	**74**	**86.5**

Note: When the percentage of sub-basin is above 50 %, it is considered significant % and is bold lettered and MI is Model Improvement
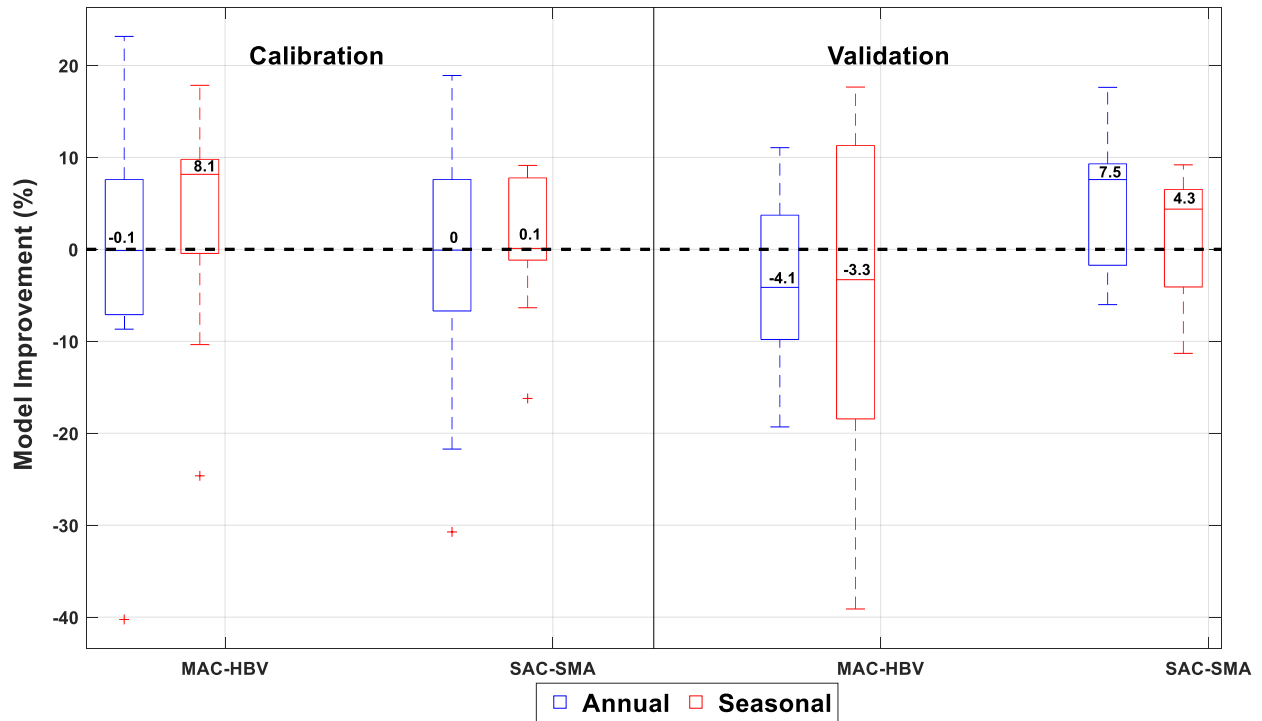
Figure 4: Model Improvement (defined by % reduction in RMSE) attained by utilizing SNOW-17 model than Degree-day method for LGRB. Positive values refer to model improvement when coupled with SNOW-17 model while negative values reveal model improvement due to implementation of Degree-day method. Boxes are delimited by the 25th and 75th percentiles, median value is printed in the boxes and the whiskers are delimited by 10th and 90th percentiles.
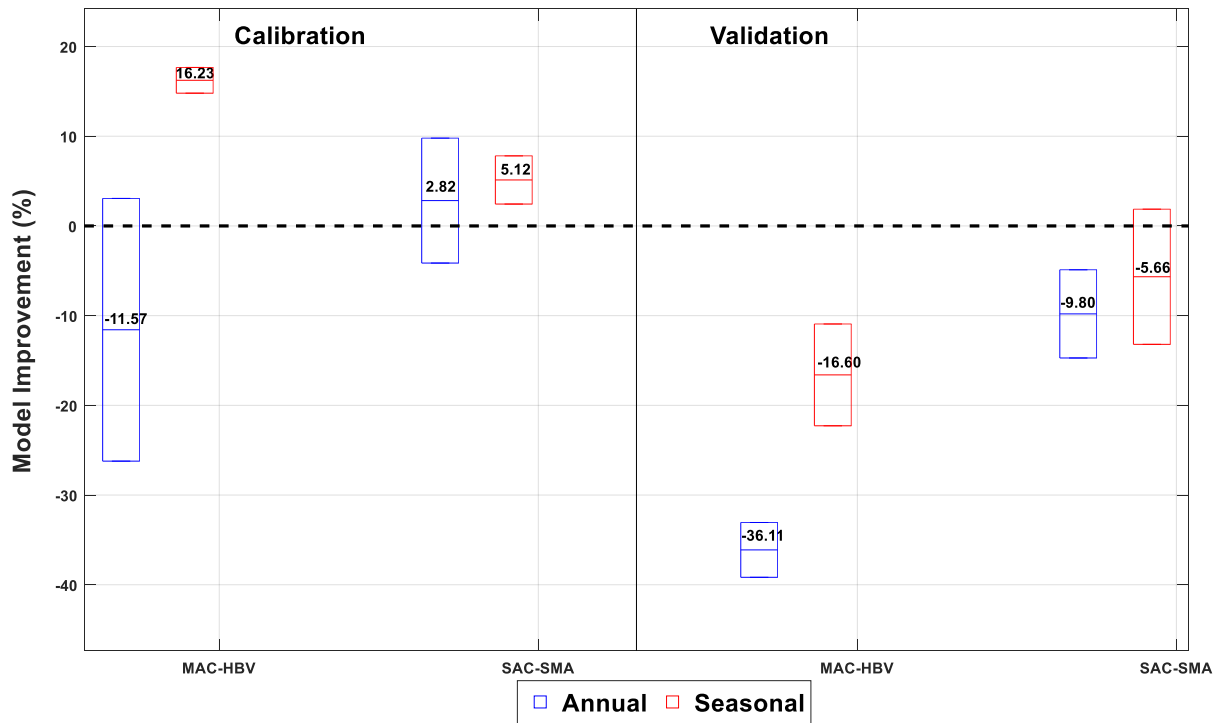
Figure 5: Model Improvement (defined by % reduction in RMSE) attained by utilizing SNOW-17 model than Degree-day method for UASR. Description is same as in Fig. 3 and as the model was calibrated at two stations, boxes here represent statistics for both the locations considered.

4.1.2 Results of Annually and Seasonally calibrated models

Spring season performance of annual and seasonal models for LGRB is presented in **Tables 2 & 3** and **Figure 6**. As shown, the mean values (Tables) of NSE and KGE and median of NSEs (**Fig.6**) for model calibration and validation period exceeds 0.5 for all the model combinations suggesting reasonable agreement between the computed and recorded reservoir inflow. Sub-basin wise performance statistics for LGRB can be found in **Appendix C.** Comparison of calibration approaches indicates that seasonal models have either identical or higher median of NSE for all the model structures during the training period (**Figure 6**). Additionally, seasonally calibrated models reveal improvement in the median of NSEs for MAC-HBV DDM (MD) and

MAC-HBV SNOW-17 (MS) models during the testing period. For example, by using seasonal models, median of NSEs increase by 11% and 5% compared with using annual MD and MS models, respectively. The model performance of UASR in terms of NSE is presented in the **Tables 4 & 5** and **Figure 7**. Sub-basin wise performance statistics for UASR can be found in **Appendix D**. Annual model optimization improves the median of NSE for MD, SAC-SMA DDM (SD) and SAC-SMA SNOW-17 (SS) models marginally when evaluated for calibration period (**Figure 7**). However, seasonal MS model provides a marked improvement in the median of NSE. In contrast, all the models calibrated for the spring season produces higher or identical NSE median values compared to yearly optimized models for the testing period. To illustrate, median of NSEs drastically increase by 56%, 17% and 28% when the seasonal MS, SD and SS models are used as compared to annual models for the validation period, respectively. In summary, comparative results suggest that out of 16 total model scenarios for the entire duration and both the study sites, 12 model scenarios produce relatively higher or equal NSE medians when seasonally optimized models are used as compared to the annually calibrated models.

Figure 8 and NRMSE in **Tables 2 & 3** show the spring peak flow performance at LGRB. Annual models perform better since marginal reduction in the median of NRMSE is obtained for the calibration and validation periods for all the model structures (**Figure 8**). Thus, Wilcoxon rank sum test for equality of medians (α=0.05) was performed to determine the statistical significance of the medians. The results found no difference between medians of NRMSE of annually and seasonally calibrated models. Interestingly, for calibration and validation periods, **Tables 2 & 3** indicates that seasonal models are as accurate as annual models in predicting the peak flows for all the model structures. Confirming with above results, nearly 55% of the sub-

basins reveal reduction in NRMSE with seasonal calibration approach than the annual optimization at LGRB for the entire study period (**Table 6**). For the second study site, UASR, NRMSE statistics are presented in **Figure 9**. It clearly indicates that median of NRMSE for seasonally calibrated MD, MS, SD and SS models show better or comparable performance to annual calibration approach during the training period and outperformed annual models for all the model combinations in the testing period. For example, with seasonally optimized MS and SS models the median of NRMSE is reduced by 16% and 40% respectively during the calibration period while it is reduced by 9% and 29% in the model testing period, respectively. Overall, majority of the sub-basins (**Table 6**) provides competitive or better performance with seasonally optimized models as opposed to annually calibrated models at both the watersheds for entire study duration.
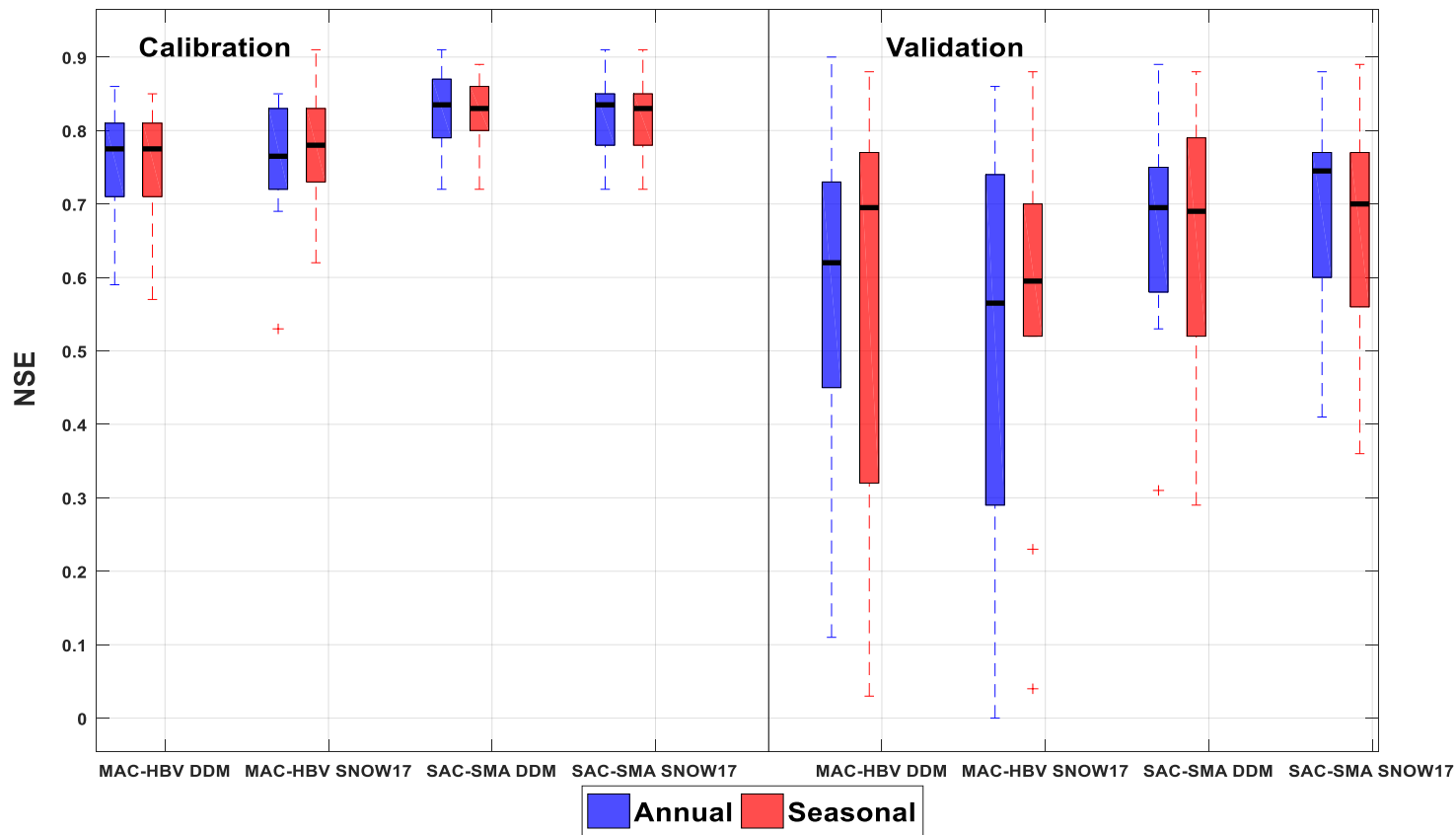
Figure 6: NSE statistics for MAC-DDM, MAC SNOW-17, SAC-DDM, SAC SNOW-17 model structures for annual and seasonal models of LGRB. Boxplot description same as fig. 3 except here median is marked with a black thick line inside boxes.

Figure 7: NSE statistics for MAC-DDM, MAC SNOW-17, SAC-DDM, SAC SNOW-17 model structures for annual and seasonal models of UASR. Boxplot description same as Fig. 4 except here median is marked with a black thick line inside boxes.

Figure 8: NRMSE statistics for MAC-DDM, MAC SNOW-17, SAC-DDM, SAC SNOW-17 model combinations for annual and seasonal models of LGRB. NRMSE is computed for spring season flows above 75 percentile. See fig. 5 for box plot description.
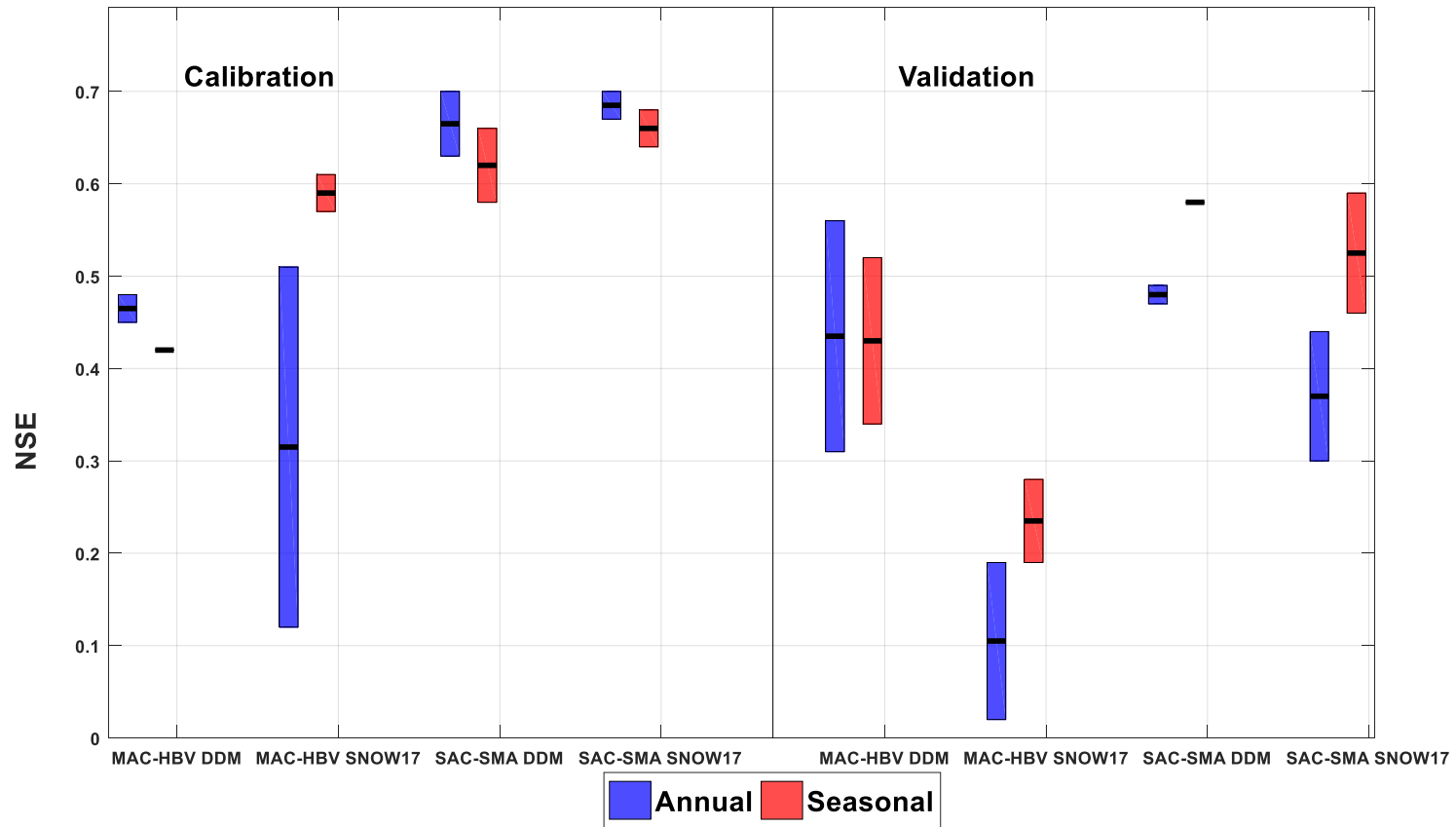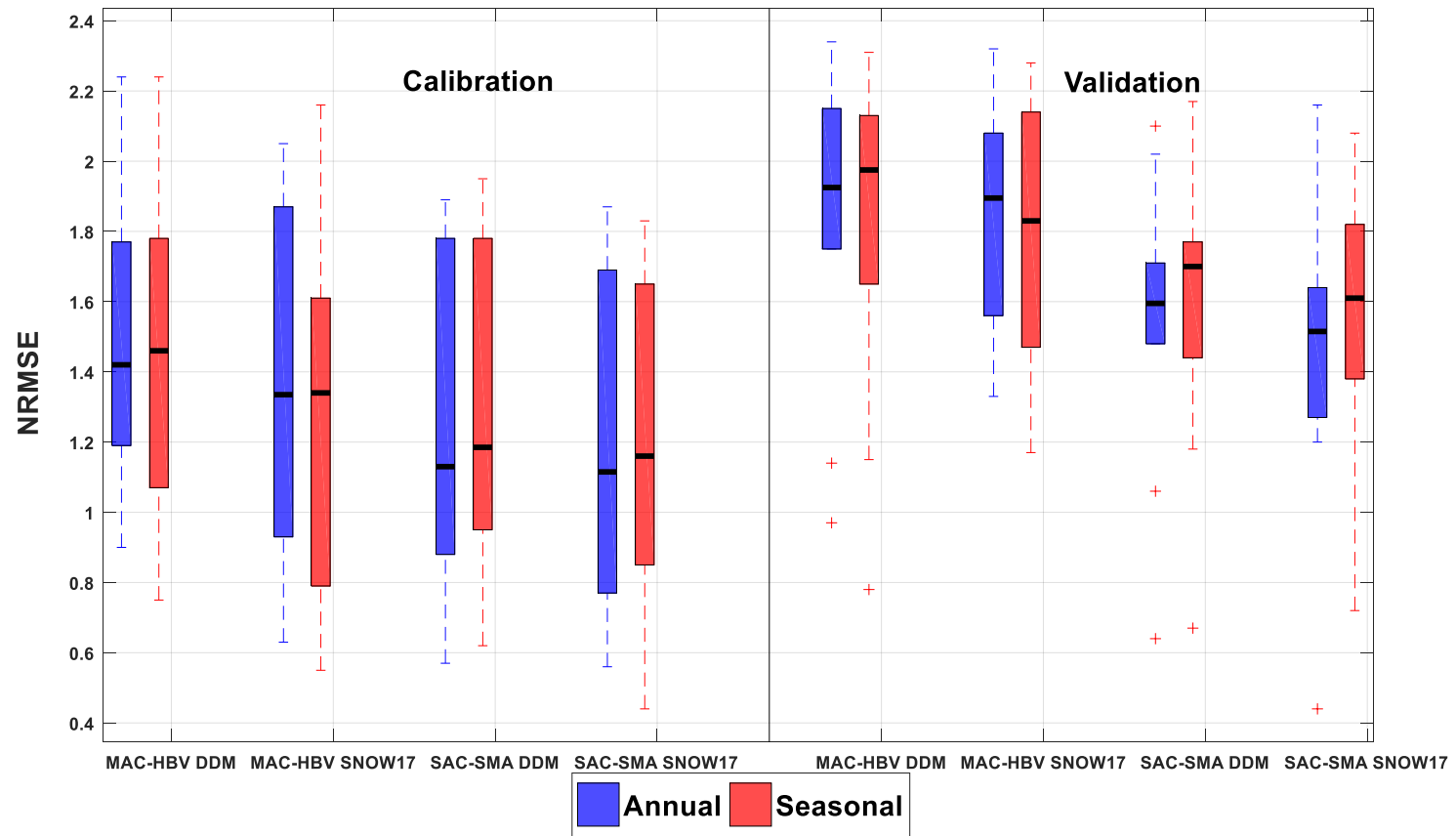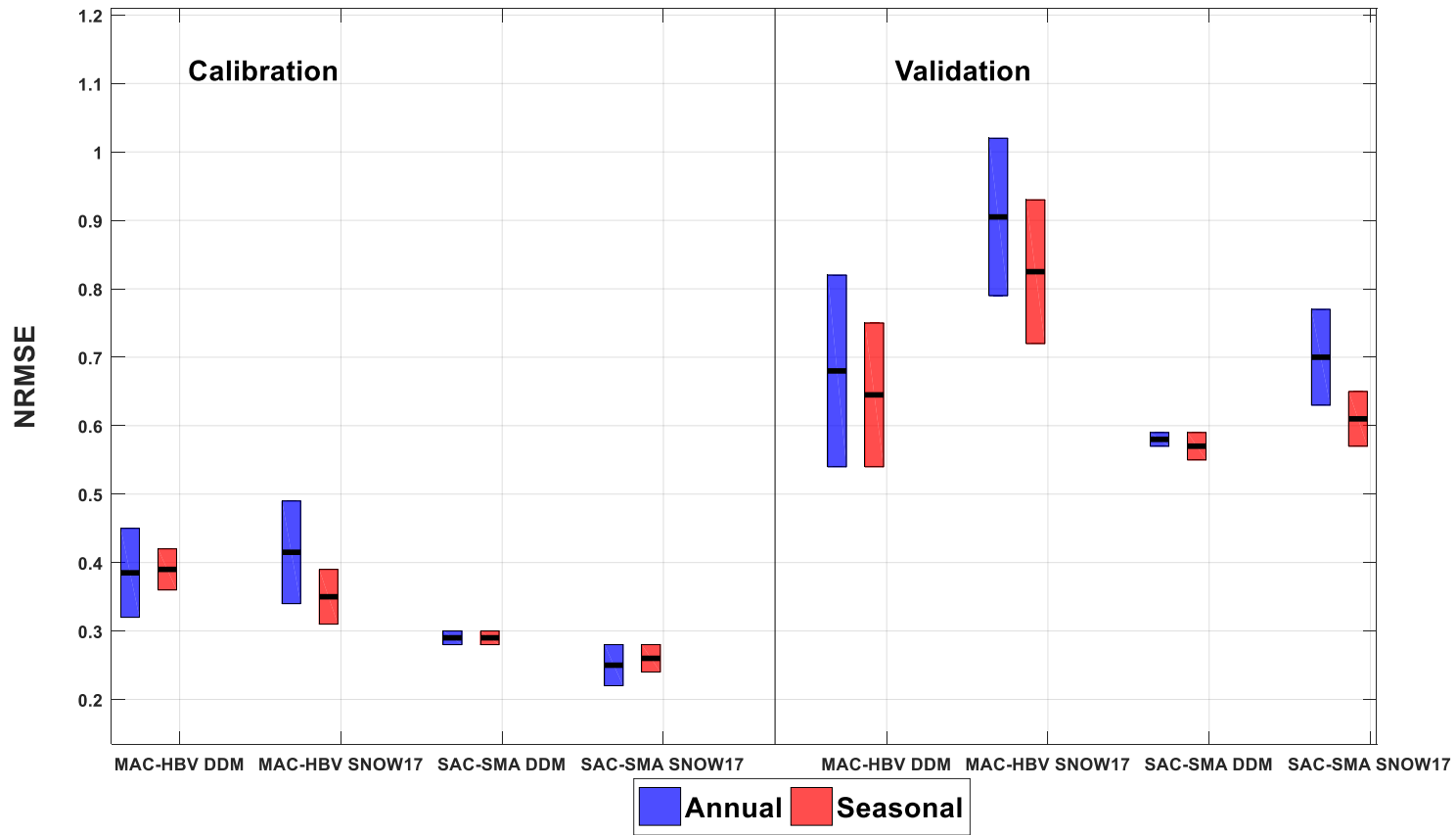
Figure 9: NRMSE statistics for MAC-DDM, MAC SNOW-17, SAC-DDM, SAC SNOW-17 model combinations for annual and seasonal models of UASR. See Fig. 6 for box plot description.

4.1.3 Comparison between Hydrological Models: MAC-HBV and SAC-SMA

Model performance of MAC-HBV and SAC-SMA hydrological models for the spring season is shown in **Figure 6** and **Tables 2 & 3**. Fig. 5 suggests that in the calibration period, SAC-SMA model combinations perform better than MAC-HBV model combinations for both the optimization approaches at LGRB. For instance, it indicates an increase in median of NSE by 43%, 54%, 47% and 11% with annually optimized SD and SS models and seasonally optimized SD and SS models during the calibration period, respectively. A similar trend was observed in the validation period but it revealed a large increase in the median of NSEs. For instance, median of NSE increased by 270% and 126% with annual and seasonal SS models as compared to MAC-HBV models, respectively. Furthermore, at UASR, NSE (**Fig. 7**) and KGE (**Table 4 & 5**) statistics suggest that SAC-SMA model outperformed during both the calibration and validation periods for most model combinations. Normalized RMSE metrics provide an accurate measure of peak flow model performance and is provided in **Figures 8 & 9** and NRMSE in **Tables 2 – 5** for both study sites. The median NRMSE at LGRB (**Fig. 8**) spans between 1.33 and 1.46 mm/day and 1.83 and 1.97 mm/day for MAC-HBV model combinations whereas it is reduced for SAC-SMA model combinations, for instance, it spans between 1.11 and 1.18 mm/day and 1.51 and 1.70 mm/day during the calibration and validation periods, respectively. With an exception of annual MS model during the training period, other model combinations have median NRMSE of SAC-SMA models consistently decreased than MAC-HBV models at UASR (**Fig. 9**). While during the validation years, median NRMSE decreased by 14%, 12%, 6% and 26% for annual and seasonal SD and SS models, respectively. Overall, whatever optimization approach or snowmelt routine is used, SAC-SMA hydrological model clearly outperformed the

MAC-HBV model performance in estimating spring season and spring peak flows at both study sites.

4.1.4 Visual Inspection of Model Performance

To further assess the general model performance, scatterplots of observed and simulated reservoir inflow are presented for the model combinations at LGRB (**Fig. 10**). As mentioned earlier, model assessment is solely based on spring season (Apr-Jun) performance. Validation plots (**Fig. 10**) reveal that annually optimized SS model lead to overestimation of reservoir inflow simulations for spring season as well as peak flows but this overestimation is less in case of seasonally optimized SS model. For instance, for the observed inflow of about 1200 cms, the simulated inflow is about 4000 cms for annually optimized model while it is about 3000 cms for seasonally optimized model. In addition, observed peak inflow of about 4600 cms was better captured by seasonal model than the annual model which overestimated the inflow to about 5200 cms. Furthermore, scatterplots for DDM model combinations fall near the ideal or 45° line for inflows less than 1000 cms and over- and under- estimation is less than scatterplots for models coupled with SNOW-17 model. For example, for MD and MS models the simulated inflow is 4700 cms and 5200 cms when the observed inflow is about 3900 cms respectively. The simulated inflow from MS model is 4000 cms for observed inflow of 4300 cms whereas this underestimation is less in case of MD model with simulated inflow of about 4250 cms. In addition, it is interesting to note that MAC-HBV model is performing very competitive to the SAC-SMA model combinations.

In order to further substantiate the model performance statistics and scatterplots discussed above, hydrographs of recorded and computed reservoir inflows are presented in **Figure 11 & 12** for the

LGRB and UASR respectively. For LGRB (**Fig.11**), seasonally optimized SAC-SMA model appears effective at simulating the magnitude and timing of the spring season inflow than annually optimized MAC-HBV and SAC-SMA models and seasonal MAC-HBV model. It also indicates that DDM is able to as accurately estimate peak flows as SNOW-17 model. Additionally, at UASR (**Fig.12**) plots clearly reveal that seasonally calibrated SAC-SMA model with DDM captures better observed peak flows and shape of the hydrograph. Other model combinations tend to either under- or over-estimate and are not able to capture the rising and falling limb of the hydrograph. Thus, overall examination of the figures at both the study sites confirms with previously obtained model performance statistics indicating the seasonal SAC-SMA model with DDM to provide improved peak flow simulations.
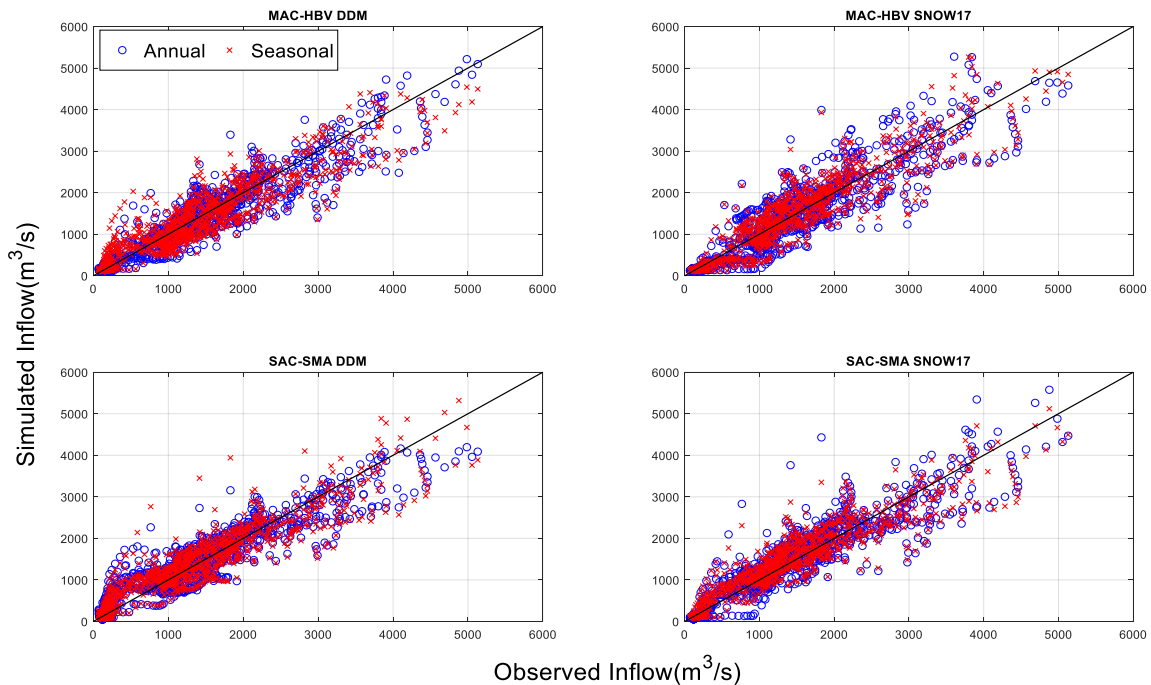
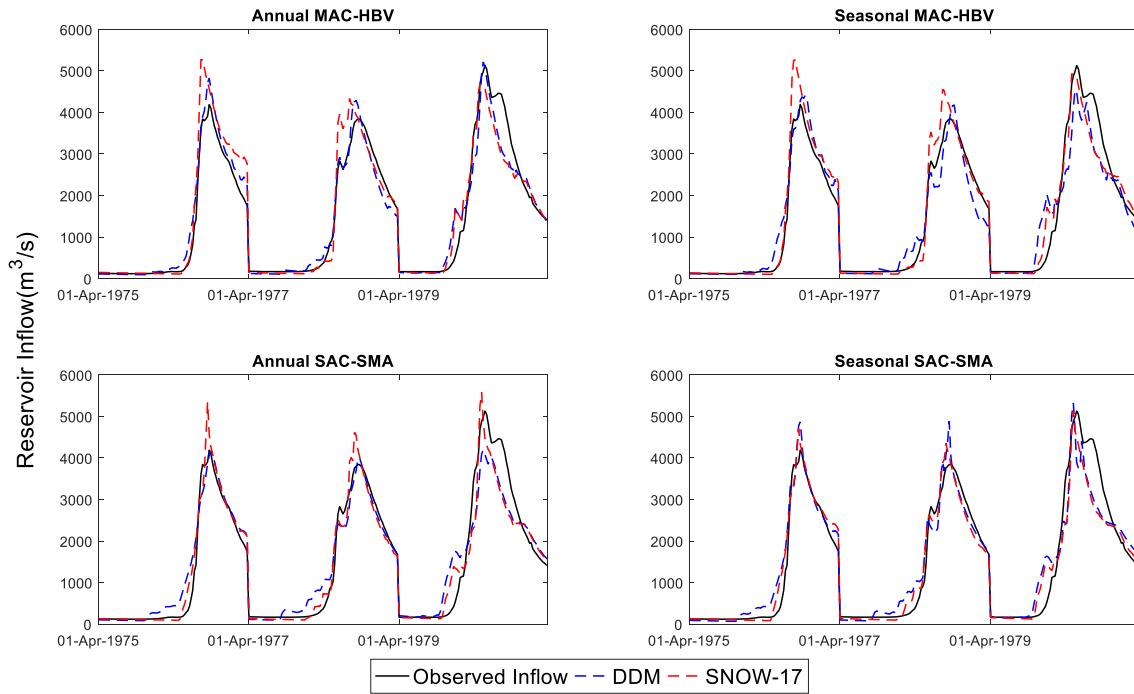**Figure 10: Validation scatterplots for spring season at LGRB**

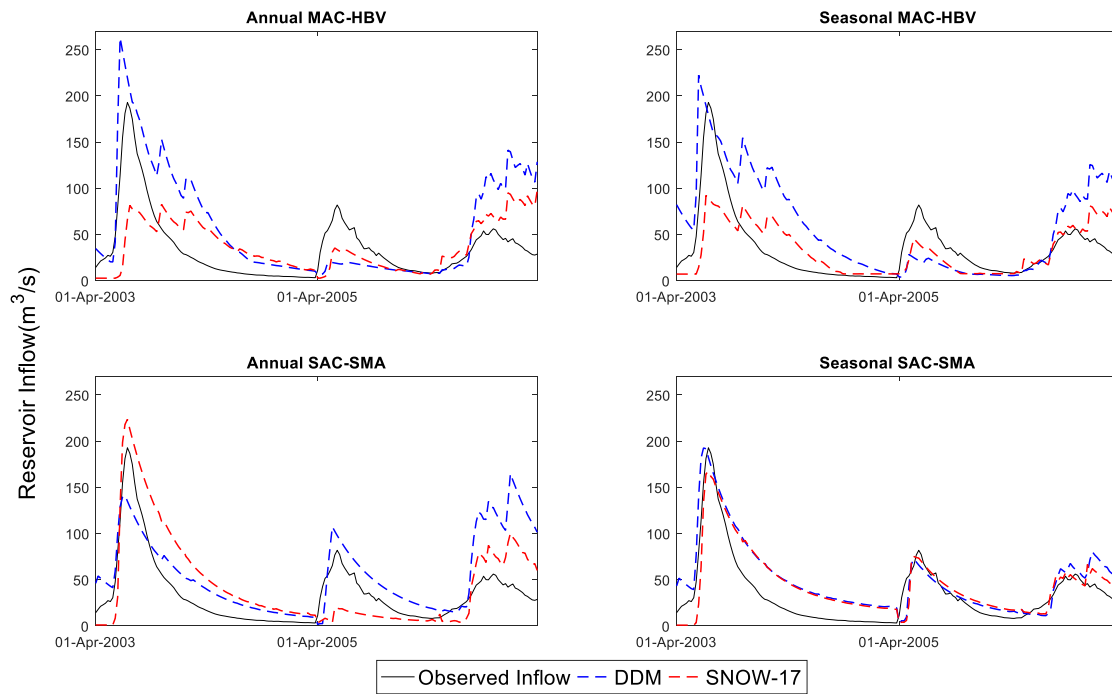**Figure 11: Hydrographs for spring season inflow simulations for LGRB**

Figure 12: Hydrographs showing spring season inflow simulations for UASR

4.2 Discussion

Snowmelt estimation is an important component of hydrologic modeling system especially for spring peak flow prediction in snow-dominated watersheds. Since most operational forecast applications use temperature index based approaches instead of energy budget models owing to the factors discussed in **sub section 1.4.4**, this study used Degree-day method and SNOW-17 model as they solely rely on temperature observations for snowmelt estimation. The reservoir inflow estimates obtained from DDM were compared to those produced by SNOW-17 model. Interestingly, the results showed that DDM has high ability to capture snowmelt driven spring floods and was found to be comparable to or better than SNOW-17 model. This study showed the flexibility of DDM in adapting to different hydrologic models and hydrological systems (Figs. 10 & 11) and providing consistently good results. Better performance of DDM may be attributed to forested and undeveloped sites used in the study where DDM has well demonstrated its ability to capture snowmelt induced peak flows (WMO, 1986). The successful application of snowmelt estimation methods at LGRB may be due to temperature being a better sole indicator of surface energy balance in forested areas since canopy diminishes the effects of direct solar radiation and wind (Melloh, 1999). Whereas, the dominant land cover in UASR is cropland(Unduche et al., 2018), so temperature may not suffice to explain the physical basis of involved snow processes leading to relatively limited performance at UASR. Although SNOW-17 model has been operational for the past few decades now, it was found in this case to be less effective to achieve accurate spring flow prediction particularly at UASR (Fig. 11). This outcome may be partially due to the watershed not considered spatially distributed or divided into elevation zones (Anderson, 2006). However, this finding is consistent with (Lundquist and

Flint, 2006) where limited performance of SNOW-17 model was demonstrated in topographically complex terrain.

Parameter optimization is an important part of the hydrologic modeling process. In case of extreme events, operational hydrologists require calibration approach that is computationally efficient and has high ability to capture the hydrological information driven by forcing data. As optimizing model parameters considering annual time series is inefficient particularly when seasonal forecasts are of interest, seasonal model calibration approach was evaluated to test its robustness against annually calibrated models in capturing the spring season reservoir inflow. Results suggested that seasonal models performed competitive and often better than annual model calibration approach at LGRB and UARB respectively (**Figs. 8 & 9**). A possible limitation of the annual calibration approach can be that it accounts for the low, medium and high flows simultaneously where most of the year-round flows are low and medium flows except the spring season flow. Thus due to high variability in the annual flow regimes, optimal model parameter estimates obtained by calibrating annually may not be very sensitive to the spring season flows. Unlike annual models, seasonal models have an advantage of being calibrated specifically to the spring season flows and thus demonstrated higher ability to capture the recorded high flows.

To facilitate inflow forecasting, hydrologic models MAC-HBV and SAC-SMA were used in the study. SAC-SMA model combinations demonstrated capability of simulating the spring peak flows consistently better than MAC-HBV models. Moreover, both hydrologic models demonstrate less accuracy at UASR than at LGRB. The limited model performance at UASR can be partially attributed to the hydrological complexity emerging out of the fill and spill of potholes in the UASR (Blais et al., 2016). Nevertheless, more accurate estimates of flow are

obtained here using conceptual models than the results obtained by (Unduche et al., 2018) where four hydrological models specifically developed for Shellmouth Reservoir inflow forecasts were evaluated for operational flood forecasting at UASR. Their results demonstrated poor performance when HSPF and HBV-EC conceptual models were assessed for the spring season.

Chapter 5 – Conclusions

5.1 Conclusions

Accurate and reliable spring flood forecasts are important for management and planning purposes. In snowmelt dominated watersheds, spring floods are strongly dependent on the amount of snowmelt runoff generated due to warm temperatures experienced during the season. Though notable efforts have been made in improving the accuracy of spring flood predictions, it still remains a challenging task due to the complexity of the hydrologic processes involved. This study explored the potential of snowmelt estimation techniques and optimization approaches to improve spring flood simulations.

Firstly, a literature review was conducted to identify the potential snowmelt estimation methods to be used in the study and was summarized in **Chapter 1**. According to the process representation involved in the snowmelt models, they were categorized into temperature index models, hybrid models and energy budget models. It was found that recent applications have shown a shift from degree-day method to energy budget approaches. However, budget models require additional data such as radiation, wind speed, relative humidity and computational resources, reducing feasibility and operational application of these methods. On the contrary, degree-day method and SNOW-17 model that solely rely on temperature to predict snowmelt were selected herein. Both methods are promising and have been widely used in hydrological applications to simulate snowmelt. Compared to degree-day method, SNOW-17 model is sophisticated, requires more computational power and is operationally used for snowmelt forecasts by NWSRFS throughout snow dominated watersheds in the United States.

A comparative analysis was performed to assess the effectiveness and accuracy of degree-day method as compared to SNOW-17 model particularly in terms of their potential to capture the spring season and peak reservoir inflows. Additionally, seasonal model calibration approach was tested against the common annual model optimization approach for enhanced spring flood simulations. Subsequently, the impacts of applying MAC-HBV and SAC-SMA hydrologic models on producing desired spring peak flow responses were evaluated. Thus, a total of 8 model configurations were obtained from a combination of two snowmelt estimation techniques, two calibration approaches and two hydrological models. The model combinations were evaluated at La-Grande River Basin (LGRB) in the Province of Quebec and Upper Assiniboine river at Shellmouth Reservoir (UASR) in the Province of Manitoba.

Analyses of the results indicate that degree-day method performed consistently better than or comparable to SNOW-17 model at both the watersheds. Moreover, flexibility and applicability of DDM was well demonstrated at the more complex terrain of UASR where SNOW-17 model was unable to accurately capture the spring peak flows. The comparison of seasonal models with annual models suggested that calibrating over spring season offers an effective alternative for improving spring peak flow prediction. Subsequently, though MAC-HBV model was very competitive to SAC-SMA hydrologic model at LGRB, more accurate estimates of flow are obtained with SAC-SMA model when coupled with whatever the snowmelt estimation technique or calibration approach at both watersheds. Overall, improved spring peak flow results are obtained by employing degree-day method and seasonally calibrated SAC-SMA model using PSO algorithm to obtain optimal model parameters. Furthermore, considerable advantage of using DDM is that it is simple and easier to implement while using seasonal models is less time-consuming with lower computational cost – hence it offers a cost-effective solution. This study

results will aid flood forecasters in selecting an effective combination of methods for operational applications.

5.2 Future Work

Despite the comparative analysis found a robust model combination, MRB statistics presented in **Appendix E** reveal that model structures underestimate spring season flows in terms of volume particularly at UASR. The calibration at UASR was conducted considering large drainage areas as single lumped sub-basin. This strategy neglects spatial variation of geophysical variables in the basin and hence it is often suggested to divide the watershed into sub-basins that separate the headwaters and local drainage areas for accuracy in prediction. Thus, further study should include dividing the watershed into smaller sub-basins. Moreover, in the study, observed SWE was not used as an input since SWE data are not readily available at most sites for operational use. Whereas snow parameter data products such as SNODAS, CMC, MODIS and others exist, their availability vary in space and time and also require exhaustive post-processing, thus limiting the feasibility of such data products. Where data are available, the potential of using observed SWE as an input to improve the spring peak flow simulations should be explored. Moreover, it would be interesting to investigate if similar findings are obtained when SWE estimations from the two snowmelt models are evaluated against observed SWE data. Since the snowmelt models used herein were temperature index models, a detailed physically based process description for energy balance can be tested for its potential to further improve simulations. Furthermore, implementation of the model structures in an urban watershed will test its applicability in different hydrological settings to learn if similar findings are obtained and should be considered for future work.(Unduche et al., 2018) mentioned that UASR is highly affected by the frozen ground effect particularly when the basin is experiencing subzero

temperatures. Release of water from frozen ground can significantly contribute to melt runoff during spring season. This implies that adding a frozen ground modeling component using a frozen ground index can lead to improved spring flow prediction accuracy. Owing to the unique hydrology of prairie region, CRHM model was specifically developed by (Pomeroy et al., 2007) to address the cold region hydrological phenomena including modules to estimate infiltration of water in frozen soils. Further research may include implementation of hydrologic model based on the unique hydrological characteristics of the watershed. Nevertheless, it will restrict the applicability of model to specific watershed.

References

Abbott, M.B., Bathurst, J.C., Cunge, J.A., O'Connell, P.E., Rasmussen, J., 1986. An introduction to the European Hydrological System — Systeme Hydrologique Europeen, "SHE", 1: History and philosophy of a physically-based, distributed modelling system. J. Hydrol. 87, 45–59. https://doi.org/10.1016/0022-1694(86)90114-9

Ahmed, S., Coulibaly, P., Tsanis, I., 2015. Improved Spring Peak-Flow Forecasting Using Ensemble Meteorological Predictions. J. Hydrol. Eng. 20, 04014044. https://doi.org/10.1061/(ASCE)HE.1943-5584.0001014

Albert, M., Krajeski, G., 1998. A fast, physically based point snowmelt model for use in distributed applications. Hydrol. Process. 12, 1809–1824. https://doi.org/10.1002/(SICI)1099-1085(199808/09)12:10/11<1809::AID-HYP696>3.0.CO;2-5

Anderson, E.A., 2006. Snow accumulation and ablation model–SNOW-17. Natl. Ocean. Atmospheric Adm. Natl. Weather Serv. Silver Springs MD.

Anderson, E.A., 1973. National Weather Service river forecast system–snow accumulation and ablation model. Tech. Memo. NWS HYDRO-17 Novemb. 1973 217 P.

Awol, F.S., Coulibaly, P., Tolson, B.A., 2018. Event-based model calibration approaches for selecting representative distributed parameters in semi-urban watersheds. Adv. Water Resour. https://doi.org/10.1016/j.advwatres.2018.05.013

Bartelt, P., Lehning, M., 2002. A physical SNOWPACK model for the Swiss avalanche warning: Part I: numerical model. Cold Reg. Sci. Technol. 35, 123–145. https://doi.org/10.1016/S0165-232X(02)00074-5

Bathurst, J.C., Cooley, K.R., 1996. Use of the SHE hydrological modelling system to investigate basin response to snowmelt at Reynolds Creek, Idaho. J. Hydrol. 175, 181–211.

Bathurst, J.C., Wicks, J.M., O'Connell, P.E., 1995. The SHE/SHESED basin scale water flow and sediment transport modelling system. Comput. Models Watershed Hydrol. 563–594.

Bergstrom, S., 1976. Development and application of a conceptual runoff model for Scandinavian catchments.

Blais, E.-L., Greshuk, J., Stadnyk, T., 2016. The 2011 flood event in the Assiniboine River Basin: causes, assessment and damages. Can. Water Resour. JournalRevue Can. Ressour. Hydr. 41, 74–84.

Bokhorst, S., Pedersen, S.H., Brucker, L., Anisimov, O., Bjerke, J.W., Brown, R.D., Ehrich, D., Essery, R.L., Heilig, A., Ingvander, S., others, 2016. Changing Arctic snow cover: A review of recent developments and assessment of future needs for observations, modelling, and impacts. Ambio 45, 516–537.

Bowling, L.C., Lettenmaier, D.P., Nijssen, B., Graham, L.P., Clark, D.B., El Maayar, M., Essery, R., Goers, S., Gusev, Y.M., Habets, F., others, 2003. Simulation of high-latitude hydrological processes in the Torne–Kalix basin: PILPS Phase 2 (e): 1: Experiment description and summary intercomparisons. Glob. Planet. Change 38, 1–30.

Brun, E., Martin, E., Simon, V., Gendre, C., Coleou, C., 1989. An energy and mass model of snow cover sidtable for operational avalanche forecasting. J. 0Glaciology 35, 1.

Burnash, R.J., Ferral, R.L., McGuire, R.A., 1973. A generalized streamflow simulation system, conceptual modeling for digital computers.

Cazorzi, F., Dalla, F.G., 1996. Snowmelt modelling by combining air temperature and a distributed radiation index. J. Hydrol. 181, 169–187.

Chang, D., Fossum, J.G., 1997. Simplified energy-balance model for pragmatic multi-dimensional device simulation. Solid-State Electron. 41, 1795–1802. https://doi.org/10.1016/S0038-1101(97)00142-1

Clyde, G.D., 1931. Snow-melting characteristics.

Collins, E., 1934. Relationship of degree-days above freezing to runoff. Eos Trans. Am. Geophys. Union 15, 624–629. https://doi.org/10.1029/TR015i002p00624-2

Coulibaly, P., 2003. Impact of meteorological predictions on real-time spring flow forecasting. Hydrol. Process. 17, 3791–3801. https://doi.org/10.1002/hyp.5168

Coulibaly, P., Bobée, B., Anctil, F., 2001. Improving extreme hydrologic events forecasting using a new criterion for artificial neural network selection. Hydrol. Process. 15, 1533–1536. https://doi.org/10.1002/hyp.445

Coulibaly, P., Keum, J., 2016. Snow Network Design and Evaluation for La Grande River Basin, Hydro-Quebec, Canada (Project No. 016-0223–24134). McMaster University.

Day, G.N., 1985. Extended Streamflow Forecasting Using NWSRFS 14.

Debele, B., Srinivasan, R., Gosain, A.K., 2010. Comparison of process-based and temperature-index snowmelt modeling in SWAT. Water Resour. Manag. 24, 1065–1088.

Devia, G.K., Ganasri, B.P., Dwarakish, G.S., 2015. A review on hydrological models. Aquat. Procedia 4, 1001–1007.

DeWalle, D.R., Henderson, Z., Rango, A., 2002. Spatial and temporal variations in snowmelt degree-day factors computed from SNOTEL data in the Upper Rio Grande basin, in: Proceedings of the Western Snow Conference, Granby, CO, USA. p. 73.

DeWalle, D.R., Rango, A., 2008. Principles of snow hydrology. Cambridge University Press.

Eberhart, R., Kennedy, J., 1995. A new optimizer using particle swarm theory, in: , Proceedings of the Sixth International Symposium on Micro Machine and Human Science, 1995. MHS '95. Presented at the , Proceedings of the Sixth International Symposium on Micro Machine and Human Science, 1995. MHS '95, pp. 39–43. https://doi.org/10.1109/MHS.1995.494215

Essery, R., 2003. Aggregated and distributed modelling of snow cover for a high-latitude basin. Glob. Planet. Change, Project for Intercomparison of Land-surface Parameterization Schemes, Phase 2(e) 38, 115–120. https://doi.org/10.1016/S0921-8181(03)00013-4

Essery, R., Morin, S., Lejeune, Y., Ménard, C.B., 2013. A comparison of 1701 snow models using observations from an alpine site. Adv. Water Resour. 55, 131–148.

Essery, R., Rutter, N., Pomeroy, J., Baxter, R., Stähli, M., Gustafsson, D., Barr, A., Bartlett, P., Elder, K., 2009. SNOWMIP2: An evaluation of forest snow process simulations. Bull. Am. Meteorol. Soc. 90, 1120–1135.

Etchevers, P., Martin, E., Brown, R., Fierz, C., Lejeune, Y., Bazile, E., Boone, A., Dai, Y.-J., Essery, R., Fernandez, A., others, 2004. Validation of the energy budget of an alpine snowpack simulated by several snow models (SnowMIP project). Ann. Glaciol. 38, 150–158.

Fang, X., Minke, A., Pomeroy, J., Brown, T., Westbrook, C., Guo, X., Guangul, S., 2007. A Review of Canadian Prairie Hydrology: Principles, Modelling and Response to Land Use and Drainage Change. Cent. Hydrol. Univ. Sask. Saskat. 35.

Finsterwalder, S., Schunk, H., 1887. Der suldenferner. Z. Dtsch. Osterreichischen Alpenvereins 18, 72–89.

Flerchinger, G.N., 2000. The simultaneous heat and water (SHAW) model: user's manual. Tech. Rep NWRC 10.

Förster, K., Meon, G., Marke, T., Strasser, U., 2014. Effect of meteorological forcing and snow model complexity on hydrological simulations in the Sieber catchment (Harz Mountains, Germany). Hydrol. Earth Syst. Sci. 18, 4703–4720.

Fortin, J.-P., Turcotte, R., Massicotte, S., Moussa, R., Fitzback, J., Villeneuve, J.-P., 2001. Distributed Watershed Model Compatible with Remote Sensing and GIS Data. I: Description of Model. J. Hydrol. Eng. 6, 91–99. https://doi.org/10.1061/(ASCE)1084-0699(2001)6:2(91)

Georgievsky, M., Takeuchi, K., Ishidaira, H., 2007. ENERGY BALANCE SNOWMELT MODELING FOR DATA-POOR BASINS. Proc. Hydraul. Eng. 51, 61–66. https://doi.org/10.2208/prohe.51.61

Gupta, H.V., Kling, H., Yilmaz, K.K., Martinez, G.F., 2009. Decomposition of the mean squared error and NSE performance criteria: Implications for improving hydrological modelling. J. Hydrol. 377, 80–91. https://doi.org/10.1016/j.jhydrol.2009.08.003

Hamlin, L., Pietroniro, A., Prowse, T., Soulis, R., Kouwen, N., 1998. Application of indexed snowmelt algorithms in a northern wetland regime. Hydrol. Process. 12, 1641–1657.

Hernández-Henríquez, M.A., Mlynowski, T.J., Déry, S.J., 2010. Reconstructing the Natural Streamflow of a Regulated River: A Case Study of La Grande Rivière, Québec, Canada. Can. Water Resour. J. Rev. Can. Ressour. Hydr. 35, 301–316. https://doi.org/10.4296/cwrj3503301

Hock, R., 2003. Temperature index melt modelling in mountain areas. J. Hydrol., Mountain Hydrology and Water Resources 282, 104–115. https://doi.org/10.1016/S0022-1694(03)00257-9

Hock, R., 1999. A distributed temperature-index ice- and snowmelt model including potential direct solar radiation. J. Glaciol. 45, 101–111. https://doi.org/10.1017/S0022143000003087

Hock, R., Holmgren, B., 2005. A distributed surface energy-balance model for complex topography and its application to Storglaciären, Sweden. J. Glaciol. 51, 25–36. https://doi.org/10.3189/172756505781829566

Horton, R.E., 1915. The melting of snow. Mon. Weather Rev. 43, 599–605.

Hottelet, C., Blažková, Š., Bičík, M., 1994. Application of the ETH Snow Model to Three Basins of Different Character in Central Europe: Paper presented at EGS XVIII General Assembly (Wiesbaden, Germany – May 1993). Hydrol. Res. 25, 113–128.

Jordan, R.E., 1990. User's guide for USACRREL one-dimensional snow temperature model (SNTHERM. 89). US Army Corps of Engineers, Cold Regions Research & Engineering Laboratory.

Koivusalo, H., Heikinheimo, M., Karvonen, T., 2001. Test of a simple two-layer parameterisation to simulate the energy balance and temperature of a snow pack. Theor. Appl. Climatol. 70, 65–79.

Krauße, T., Cullmann, J., Saile, P., Schmitz, G.H., 2012. Robust multi-objective calibration strategies – possibilities for improving flood forecasting. Hydrol Earth Syst Sci 16, 3579–3606. https://doi.org/10.5194/hess-16-3579-2012

Kumar, M., Marks, D., Dozier, J., Reba, M., Winstral, A., 2013. Evaluation of distributed hydrologic impacts of temperature-index and energy-based snow models. Adv. Water Resour. 56, 77–89. https://doi.org/10.1016/j.advwatres.2013.03.006

Kustas, Remko Uijlenhoet, Albert Rango, 1994. A simple energy budget algorithm for the snowmelt runoff model. Water Resour. Res. 30, 1515–1527. https://doi.org/10.1029/94WR00152

Kuusisto, E., 1980. On the values and variability of degree-day melting factor in Finland. Hydrol. Res. 11, 235–242.

Linsley, R.K., 1943. A simple procedure for the day-to-day forecasting of runoff from snow-melt. Eos Trans. Am. Geophys. Union 24, 62–67.

Lundquist, J.D., Flint, A.L., 2006. Onset of Snowmelt and Streamflow in 2004 in the Western United States: How Shading May Affect Spring Streamflow Timing in a Warmer World. J. Hydrometeorol. 7, 1199–1217. https://doi.org/10.1175/JHM539.1

Magnusson, J., Wever, N., Essery, R., Helbig, N., Winstral, A., Jonas, T., 2015a. Evaluating snow models with varying process representations for hydrological applications. Water Resour. Res. 51, 2707–2723. https://doi.org/10.1002/2014WR016498

Magnusson, J., Wever, N., Essery, R., Helbig, N., Winstral, A., Jonas, T., 2015b. Evaluating snow models with varying process representations for hydrological applications. Water Resour. Res. 51, 2707–2723.

Mahanama, S., Livneh, B., Koster, R., Lettenmaier, D., Reichle, R., 2011. Soil Moisture, Snow, and Seasonal Streamflow Forecasts in the United States. J. Hydrometeorol. 13, 189–203. https://doi.org/10.1175/JHM-D-11-046.1

Marks, D., Domingo, J., Susong, D., Link, T., Garen, D., 1999. A spatially distributed energy balance snowmelt model for application in mountain basins. Hydrol. Process. 13, 1935–1959.

Marks, D., Kimball, J., Tingey, D., Link, T., 1998. The sensitivity of snowmelt processes to climate conditions and forest cover during rain-on-snow: a case study of the 1996 Pacific Northwest flood. Hydrol. Process. 12, 1569–1587. https://doi.org/10.1002/(SICI)1099-1085(199808/09)12:10/11<1569::AID-HYP682>3.0.CO;2-L

Markstrom, S., R. Steven Regan, Lauren Hay, Roland J. Viger, Richard M.T. Webb, Robert A.Payn, Jacob H. Lafontaine, 2015. PRMS-IV, the Precipitation-Runoff Modeling System, Version 4 (Techniques and Methods).

Martinec, J., 1975. Snowmelt-runoff model for streamflow forecasts. Nord. Hydrol. 145–154.

Martinec, J., 1960. The degree-day factor for snowmelt runoff forecasting. IUGG Gen. Assem. Hels. IAHS Comm. Surf. Waters 468–477.

Melloh, R.A., 1999. A Synopsis and Comparison of Selected Snowmelt Algorithms 23.

Moghadas, S., Gustafsson, A.-M., Muthanna, T.M., Marsalek, J., Viklander, M., 2016. Review of models and procedures for modelling urban snowmelt. Urban Water J. 13, 396–411. https://doi.org/10.1080/1573062X.2014.993996

Neitsch, S.L., Arnold, J.G., Kiniry, J.R., Williams, J.R., 2005. Soil And Water Assessment Tool Theoretical Documentation 494.

Ohmura, A., 2001. Physical Basis for the Temperature-Based Melt-Index Method. J. Appl. Meteorol. 40, 753–761. https://doi.org/10.1175/1520-0450(2001)040<0753:PBFTTB>2.0.CO;2

Pellicciotti, F., Brock, B., Strasser, U., Burlando, P., Funk, M., Corripio, J., 2005. An enhanced temperature-index glacier melt model including the shortwave radiation balance: development and testing for Haut Glacier d'Arolla, Switzerland. J. Glaciol. 51, 573–587. https://doi.org/10.3189/172756505781829124

Pomeroy, J., Boer, D.de, Martz,L.W., 2005. Hydrology and Water Resources of Saskatchewan. Cent. Hydrol. Univ. Sask. Saskat. 25.

Pomeroy, J.W., Gray, D.M., Brown, T., Hedstrom, N.R., Quinton, W.L., Granger, R.J., Carey, S.K., 2007. The cold regions hydrological model: a platform for basing process representation and model structure on physical evidence. Hydrol. Process. 21, 2650–2667.

Raleigh, M.S., Lundquist, J.D., 2012. Comparing and combining SWE estimates from the SNOW-17 model using PRISM and SWE reconstruction. Water Resour. Res. 48.

Rango, A., Martinec, J., 1995. Revisiting the degree-day method for snowmelt computations. JAWRA J. Am. Water Resour. Assoc. 31, 657–669.

Rango, A., Martinec, J., Roberts, R., 2008. Relative importance of glacier contributions to water supply in a changing climate. World Resour. Rev. 20, 233–251.

Razavi, T., Coulibaly, P., 2017. An evaluation of regionalization and watershed classification schemes for continuous daily streamflow prediction in ungauged watersheds. Can. Water Resour. JournalRevue Can. Ressour. Hydr. 42, 2–20.

Razavi, T., Coulibaly, P., 2016. Improving streamflow estimation in ungauged basins using a multi-modelling approach. Hydrol. Sci. J. 61, 2668–2679. https://doi.org/10.1080/02626667.2016.1154558

Reed, S., Koren, V., Smith, M., Zhang, Z., Moreda, F., Seo, D.-J., DMIP Participants, and, 2004. Overall distributed model intercomparison project results. J. Hydrol., The Distributed Model Intercomparison Project (DMIP) 298, 27–60. https://doi.org/10.1016/j.jhydrol.2004.03.031

Rutter, N., Essery, R., Pomeroy, J., Altimir, N., Andreadis, K., Baker, I., Barr, A., Bartlett, P., Boone, A., Deng, H., others, 2009. Evaluation of forest snow processes models (SnowMIP2). J. Geophys. Res. Atmospheres 114.

Samuel, J., Coulibaly, P., Metcalfe, R.A., 2012. Identification of rainfall–runoff model for improved baseflow estimation in ungauged basins. Hydrol. Process. 26, 356–366. https://doi.org/10.1002/hyp.8133

Samuel, J., Coulibaly, P., Metcalfe, R.A., 2011. Estimation of continuous streamflow in Ontario ungauged basins: comparison of regionalization methods. J. Hydrol. Eng. 16, 447–459.

Scheider, W.A., Logan, L.A., Geobel, M.J., 1983. A comparison of two models to predict snowmelt in Muskoka-Haliburton, Ontario, in: Proceedings of the Eastern Snow Conference. pp. 157–168.

Shamir, E., Georgakakos, K.P., 2006. Distributed snow accumulation and ablation modeling in the American River basin. Adv. Water Resour. 29, 558–570. https://doi.org/10.1016/j.advwatres.2005.06.010

Sharma, M., Coulibaly, P., Dibike, Y., 2010. Assessing the need for downscaling RCM data for hydrologic impact study. J. Hydrol. Eng. 16, 534–539.

Shrestha, R.R., Dibike, Y.B., Prowse, T.D., 2012. Modeling Climate Change Impacts on Hydrology and Nutrient Loading in the Upper Assiniboine Catchment1. JAWRA J. Am. Water Resour. Assoc. 48, 74–89. https://doi.org/10.1111/j.1752-1688.2011.00592.x

Speers, D.D., 1995. SSARR model. Comput. Models Watershed Hydrol. 367–394.

Strasser, U., Etchevers, P., Lejeune, Y., 2002. Inter-Comparison of two Snow Models with Different Complexity using Data from an Alpine Site: Selected paper from EGS General Assembly, Nice, April-2000 (Symposium OA36). Hydrol. Res. 33, 15–26.

Strasser, U., Marke, T., 2010. ESCIMO. spread–a spreadsheet-based point snow surface energy balance model to calculate hourly snow water equivalent and melt rates for historical and changing climate conditions. Geosci. Model Dev. 3, 643–652.

Tarboton, D.G., Luce, C.H., 1996. Utah energy balance snow accumulation and melt model (UEB). Citeseer.

Todd, W.M., Brooks, E.S., McCool, D.K., King, L.G., Molnau, M., Boll, J., 2005. Process-based snowmelt modeling: does it require more input data than temperature-index modeling? J. Hydrol. 300, 65–75. https://doi.org/10.1016/j.jhydrol.2004.05.002

Troin, M., Arsenault, R., Brissette, F., 2015. Performance and Uncertainty Evaluation of Snow Models on Snowmelt Flow Simulations over a Nordic Catchment (Mistassibi, Canada). Hydrology 2, 289–317. https://doi.org/10.3390/hydrology2040289

Unduche, F., Tolossa, H., Senbeta, D., Zhu, E., 2018. Evaluation of four hydrological models for operational flood forecasting in a Canadian Prairie watershed. Hydrol. Sci. J.

USACE, 1998. Runoff from Snowmelt (Manual No. 1110-2–1406).

Valeo, C., Ho, C.L.I., 2004. Modelling urban snowmelt runoff. J. Hydrol. 299, 237–251.

Vehvilainen, B., 1992. Snow cover models in operational watershed forecasting. Natl. Board Waters Environ. Finl. 11.

Vrugt, J.A., Gupta, H.V., Nualláin, B., Bouten, W., 2006. Real-Time Data Assimilation for Operational Ensemble Streamflow Forecasting. J. Hydrometeorol. 7, 548–565. https://doi.org/10.1175/JHM504.1

WMO, 1986. Intercomparisons of Models of Snowmelt Runoff (No. 23), Operational Hydrology. World Meteorological Organization, Geneva, Switzerland.

Appendix A: Sub-basin information for watersheds used in study

LGRB

Sub-basin	Area (sq. km.)	Elevation (masl)	Latitude	Longitude
Caniapiscau	37328	565	53.91	-68.60
La-Forge-1	9104	452	54.38	-71.55
La-Grande-4	28443	517	53.55	-70.93
La-Grande-3	28492	428	53.45	-73.90
La-Grande-2	31148	217	54.08	-76.29
La-Grande-1	2132	141	53.78	-77.83
Eastmain-1	25857	469	52.26	-72.69
Lac-Opinaca	14401	312	52.60	-75.46
Lac-Mesgouez	10275	365	51.29	-74.36
Lac-Mistassini	18252	490	51.19	-72.88

UASR

Basin	Area (sq. km.)	Elevation (masl)	Latitude	Longitude
Kamsack	13042	539	51.59	-102.58
Shellmouth Reservoir	18330	546	51.58	-102.41

Appendix B: Sample hydrographs showing performance with NVE and Modified NVE
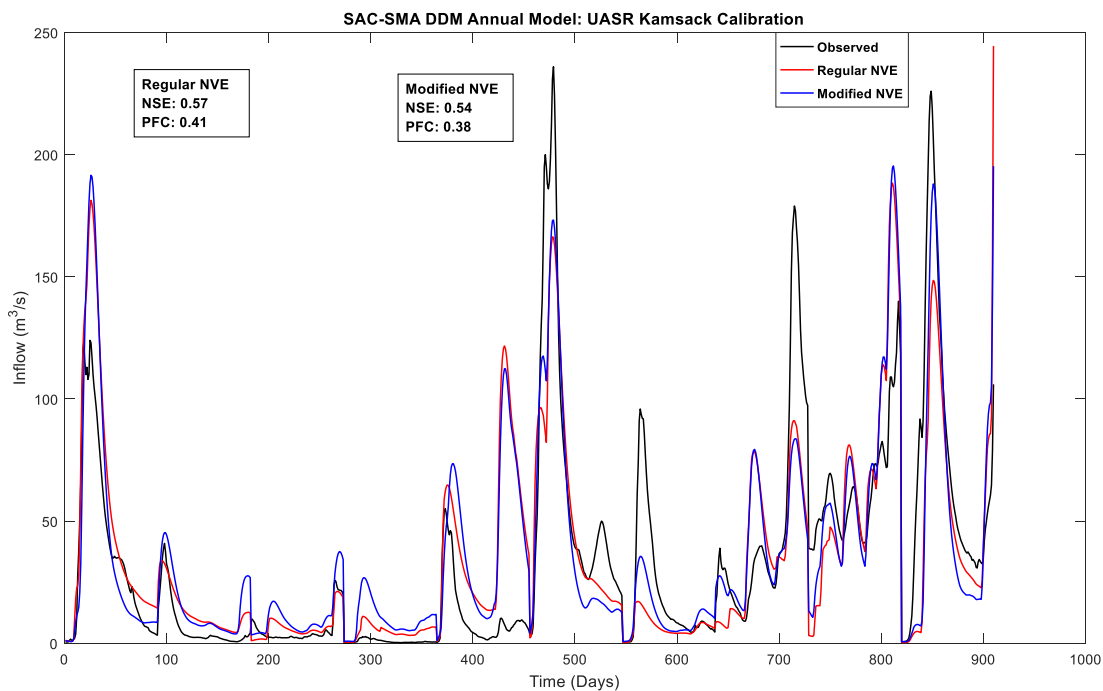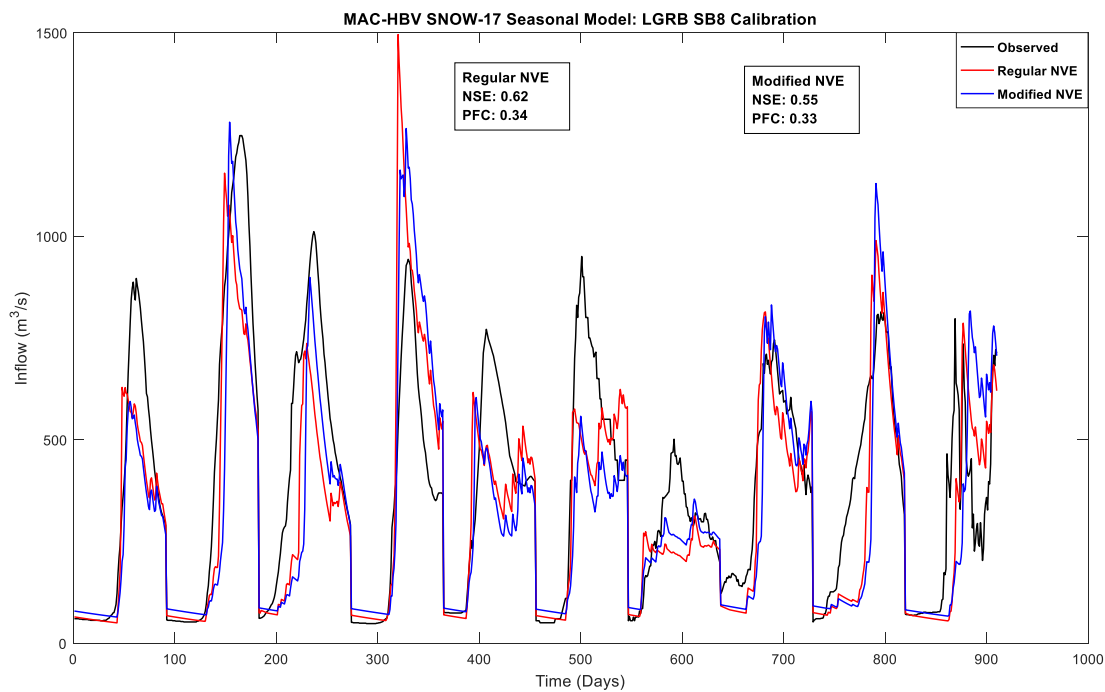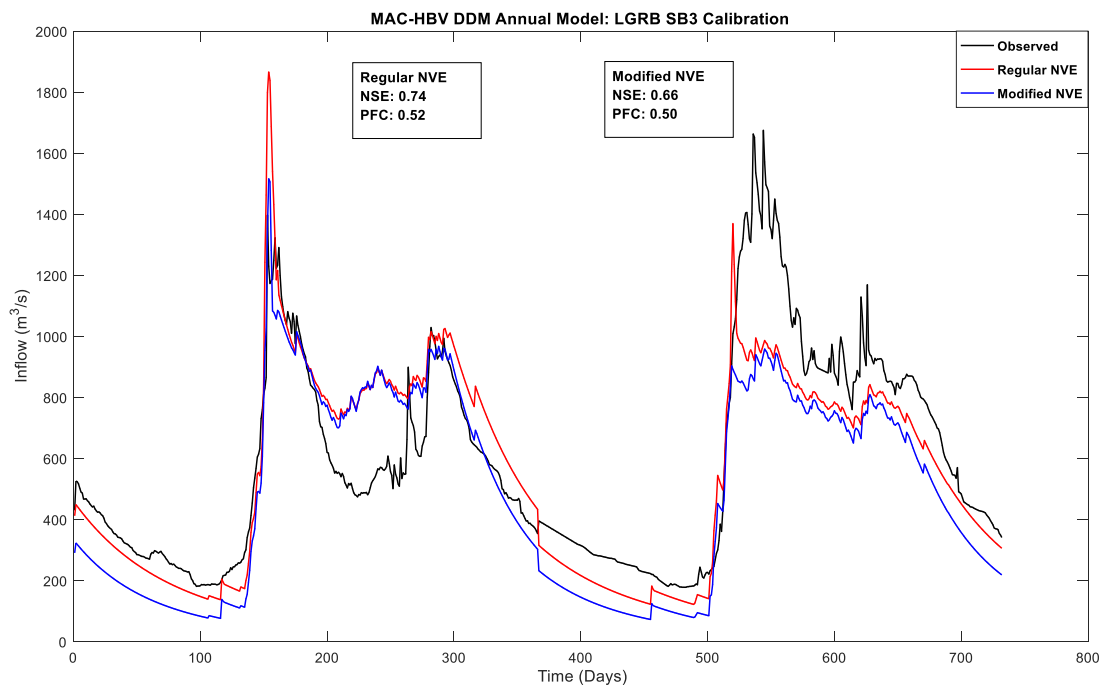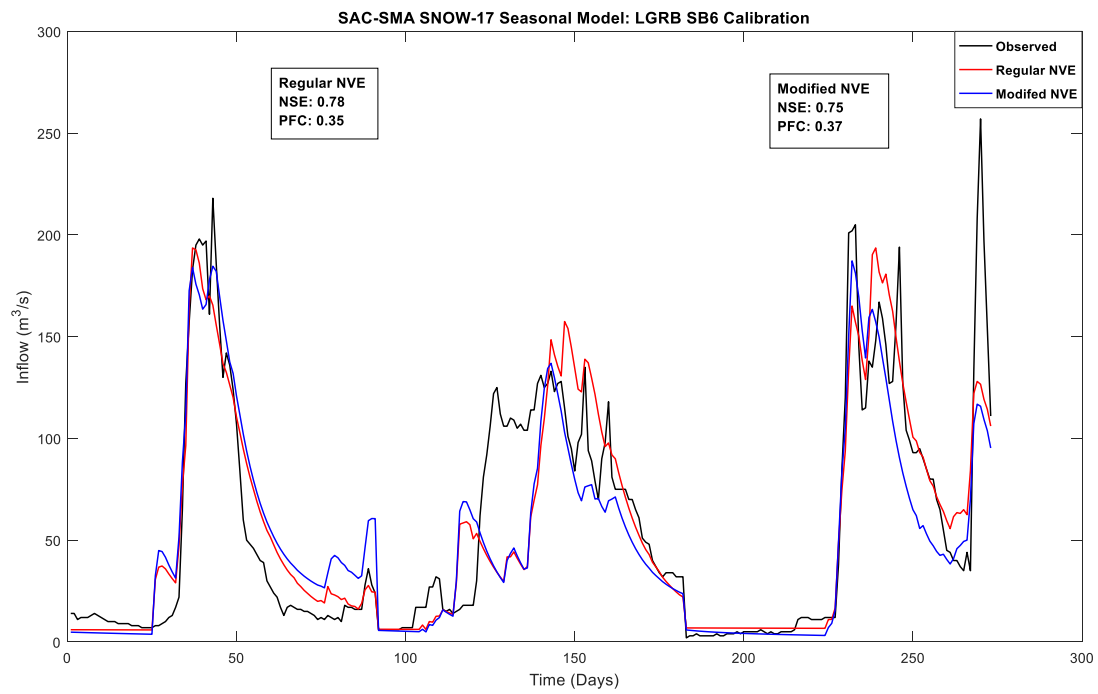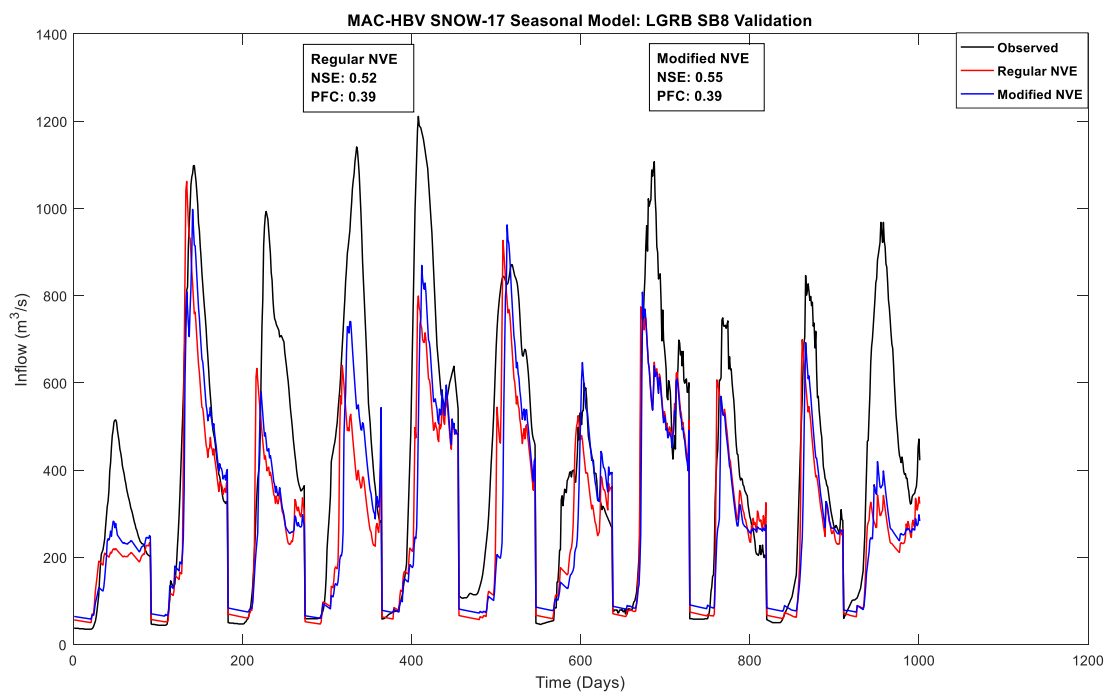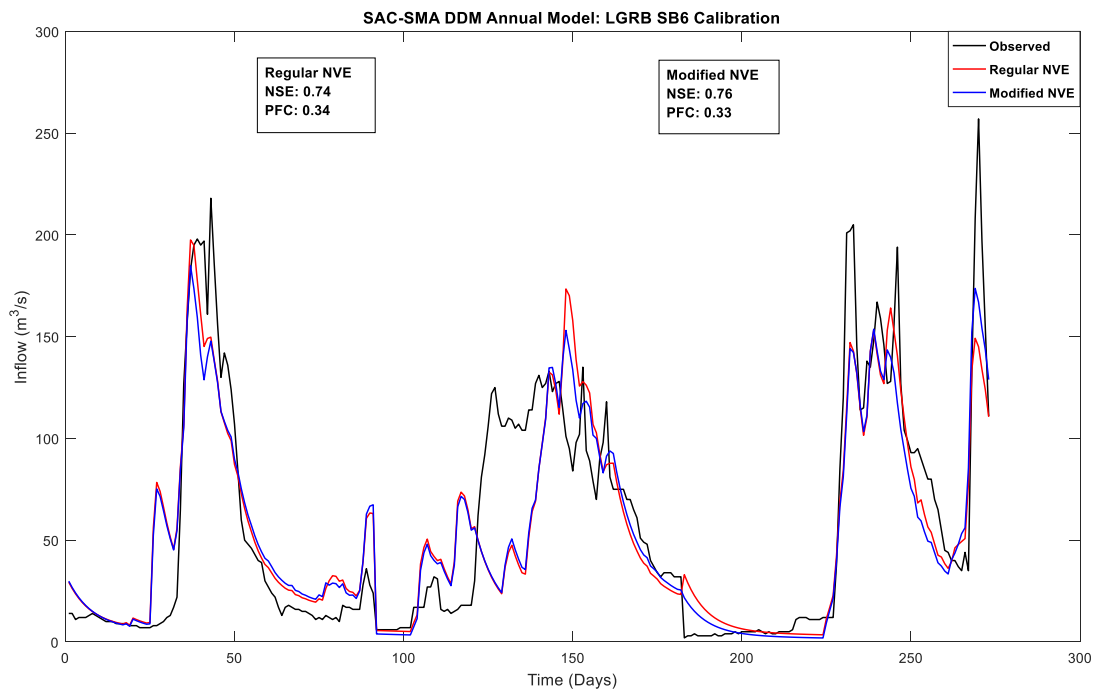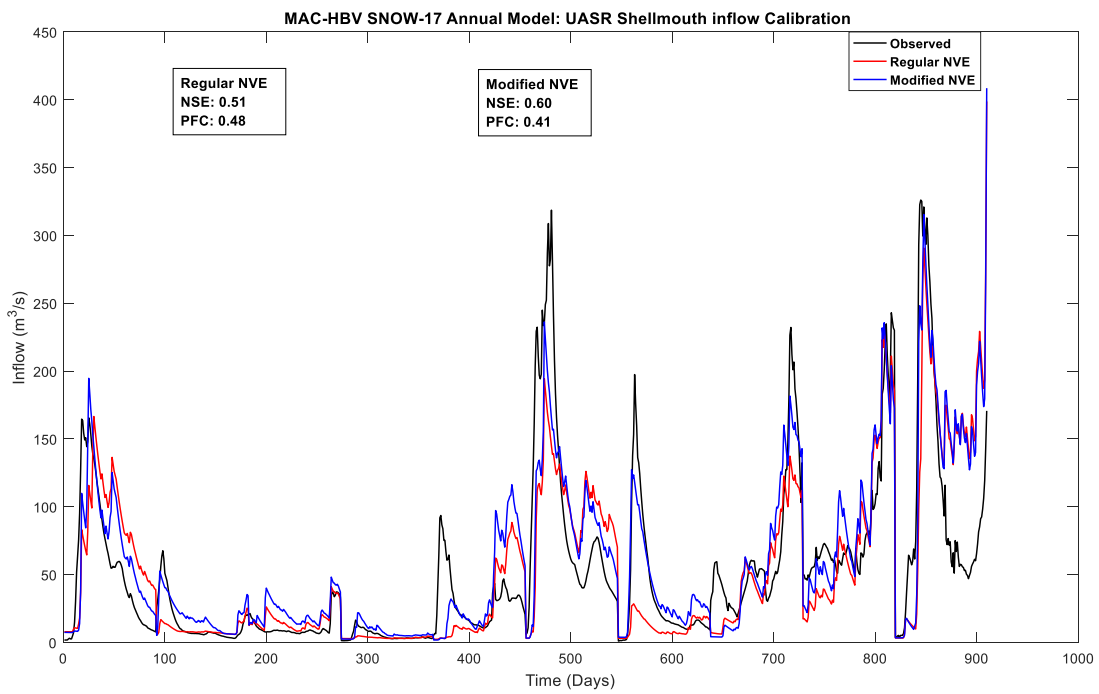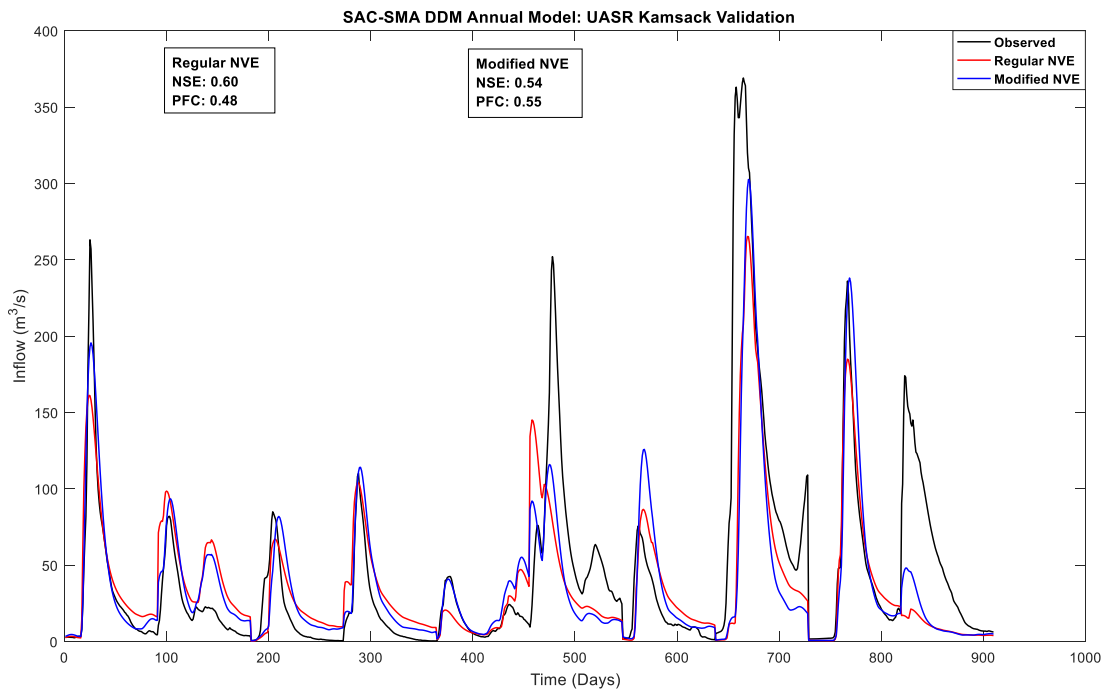
Appendix C: Sub-basin wise model performance statistics at LGRB

Sub-basin wise CALIBRATION performance statistics for ANNUAL MAC-HBV models at LGRB

| | *MAC-HBV DDM* | | | | | *MAC-HBV SNOW17* | | | | | |
Sub-basin	NSE	MRB	NVE	KGE	PFC	NSE	MRB	NVE	KGE	PFC	Model Improvement (%)
Caniapiscau	0.81	-0.01	0.78	0.87	0.30	0.83	-0.02	0.80	0.89	0.28	3.26
La-Forge-1	0.83	0.00	0.79	0.91	0.46	0.81	-0.19	0.76	0.88	0.52	-6.93
La-Grande-4	0.79	-0.11	0.72	0.83	0.53	0.75	-0.07	0.69	0.86	0.71	-8.68
La-Grande-3	0.81	-0.05	0.77	0.83	0.52	0.83	-0.05	0.82	0.90	0.45	7.59
La-Grande-2	0.76	-0.07	0.73	0.83	0.36	0.78	-0.04	0.77	0.87	0.36	4.24
La-Grande-1	0.69	-0.06	0.65	0.77	0.50	0.74	-0.06	0.71	0.82	0.45	8.54
Eastmain-1	0.71	-0.09	0.69	0.83	0.28	0.69	-0.11	0.66	0.81	0.28	-3.52
Lac-Opinaca	0.59	-0.13	0.58	0.76	0.33	0.53	-0.15	0.52	0.74	0.33	-7.10
Lac-Mesgouez	0.86	-0.05	0.80	0.88	0.27	0.72	-0.11	0.64	0.74	0.53	-40.25
Lac-Mistassini	0.75	-0.12	0.72	0.82	0.43	0.85	-0.07	0.82	0.88	0.08	23.16

Note: The aforementioned performance criteria are evaluated for spring season only

Sub-basin wise CALIBRATION performance statistics for SEASONAL MAC-HBV models at LGRB

Sub-basin	*MAC-HBV DDM*					*MAC-HBV SNOW17*					
	NSE	MRB	NVE	KGE	PFC	NSE	MRB	NVE	KGE	PFC	Model Improvement (%)
Caniapiscau	0.80	0.00	0.76	0.84	0.32	0.83	0.00	0.80	0.91	0.27	7.22
La-Forge-1	0.85	0.00	0.82	0.91	0.38	0.82	-0.03	0.78	0.90	0.45	-10.36
La-Grande-4	0.82	-0.06	0.78	0.89	0.56	0.91	-0.03	0.89	0.93	0.38	11.21
La-Grande-3	0.81	-0.10	0.78	0.86	0.40	0.87	-0.07	0.84	0.89	0.44	17.84
La-Grande-2	0.76	-0.05	0.72	0.87	0.29	0.76	-0.11	0.73	0.84	0.30	-0.44
La-Grande-1	0.67	-0.13	0.64	0.73	0.43	0.73	-0.07	0.69	0.80	0.46	9.26
Eastmain-1	0.71	-0.07	0.70	0.84	0.25	0.77	-0.02	0.74	0.88	0.28	9.79
Lac-Opinaca	0.57	-0.14	0.55	0.75	0.34	0.62	-0.30	0.58	0.77	0.36	6.03
Lac-Mesgouez	0.79	-0.14	0.74	0.82	0.45	0.67	-0.14	0.66	0.77	0.46	-24.63
Lac-Mistassini	0.74	-0.11	0.71	0.83	0.46	0.79	-0.10	0.76	0.85	0.10	9.10

Sub-basin wise VALIDATION performance statistics for ANNUAL MAC-HBV models at LGRB

Sub-basin	*MAC-HBV DDM*					*MAC-HBV SNOW17*					Model Improvement (%)
	NSE	MRB	NVE	KGE	PFC	NSE	MRB	NVE	KGE	PFC	
Caniapiscau	0.90	-0.03	0.89	0.92	0.25	0.86	-0.01	0.84	0.92	0.24	-19.31
La-Forge-1	0.61	-0.12	0.58	0.63	0.49	0.58	-0.19	0.55	0.60	0.51	-4.38
La-Grande-4	0.63	-0.11	0.59	0.72	0.57	0.29	-0.18	0.24	0.58	0.71	-18.48
La-Grande-3	0.45	-0.19	0.42	0.46	0.54	0.49	-0.25	0.47	0.51	0.54	3.72
La-Grande-2	0.67	-0.13	0.61	0.57	0.50	0.74	-0.11	0.69	0.65	0.49	11.06
La-Grande-1	0.78	0.08	0.71	0.76	0.46	0.77	0.04	0.73	0.79	0.48	-2.41
Eastmain-1	0.73	-0.16	0.71	0.75	0.32	0.69	-0.19	0.67	0.74	0.34	-6.72
Lac-Opinaca	0.56	-0.29	0.56	0.55	0.38	0.55	-0.30	0.52	0.56	0.38	-3.89
Lac-Mesgouez	0.11	-0.27	0.07	0.88	0.61	0.28	-0.16	0.19	0.64	0.53	10.27
Lac-Mistassini	0.16	-0.29	0.21	0.53	0.47	0.00	-0.16	0.06	0.50	0.32	-9.80

Sub-basin wise VALIDATION performance statistics for SEASONAL MAC-HBV models at LGRB

	MAC-HBV DDM					*MAC-HBV SNOW17*					
Sub-basin	**NSE**	**MRB**	**NVE**	**KGE**	**PFC**	**NSE**	**MRB**	**NVE**	**KGE**	**PFC**	**Model Improvement (%)**
Caniapiscau	0.88	-0.02	0.87	0.91	0.24	0.88	0.00	0.87	0.93	0.24	0.56
La-Forge-1	0.69	-0.10	0.66	0.75	0.46	0.63	-0.15	0.60	0.71	0.46	-8.45
La-Grande-4	0.77	-0.11	0.76	0.80	0.45	0.56	-0.17	0.53	0.56	0.66	-39.11
La-Grande-3	0.30	-0.38	0.25	0.38	0.57	0.52	-0.22	0.50	0.61	0.48	17.65
La-Grande-2	0.71	-0.13	0.66	0.65	0.48	0.70	-0.21	0.66	0.61	0.49	-0.65
La-Grande-1	0.79	-0.05	0.73	0.75	0.47	0.66	0.08	0.63	0.70	0.50	-26.67
Eastmain-1	0.70	-0.14	0.69	0.76	0.34	0.78	-0.10	0.75	0.84	0.31	14.33
Lac-Opinaca	0.57	-0.28	0.55	0.55	0.39	0.52	-0.30	0.49	0.52	0.39	-5.95
Lac-Mesgouez	0.32	-0.30	0.26	0.54	0.57	0.04	-0.09	0.06	0.55	0.56	-18.44
Lac-Mistassini	0.03	-0.32	0.09	0.44	0.18	0.23	-0.20	0.25	0.56	0.36	11.29

Sub-basin wise CALIBRATION performance statistics for ANNUAL SAC-SMA models at LGRB

	SAC-SMA DDM					*SAC-SMA SNOW17*					
Sub-basin	**NSE**	**MRB**	**NVE**	**KGE**	**PFC**	**NSE**	**MRB**	**NVE**	**KGE**	**PFC**	**Model Improvement (%)**
Caniapiscau	0.79	0.04	0.74	0.82	0.33	0.83	0.00	0.79	0.88	0.29	8.72
La-Forge-1	0.85	0.01	0.82	0.89	0.36	0.84	-0.02	0.81	0.90	0.41	-1.30
La-Grande-4	0.89	0.00	0.87	0.91	0.41	0.85	-0.06	0.82	0.90	0.48	-21.72
La-Grande-3	0.87	-0.01	0.85	0.89	0.41	0.87	-0.03	0.86	0.90	0.39	0.14
La-Grande-2	0.82	-0.01	0.78	0.84	0.40	0.83	-0.06	0.80	0.88	0.34	2.97
La-Grande-1	0.74	-0.03	0.70	0.77	0.44	0.78	-0.05	0.74	0.83	0.47	7.60
Eastmain-1	0.79	0.00	0.78	0.87	0.25	0.76	-0.03	0.75	0.86	0.25	-6.70
Lac-Opinaca	0.72	-0.02	0.71	0.82	0.31	0.72	-0.05	0.71	0.83	0.31	-0.31
Lac-Mesgouez	0.91	-0.02	0.89	0.93	0.42	0.85	-0.06	0.82	0.84	0.52	-30.73
Lac-Mistassini	0.86	-0.08	0.84	0.91	0.21	0.91	-0.03	0.89	0.93	0.25	18.91

Sub-basin wise CALIBRATION performance statistics for SEASONAL SAC-SMA models at LGRB

	SAC-SMA DDM					*SAC-SMA SNOW17*					
Sub-basin	**NSE**	**MRB**	**NVE**	**KGE**	**PFC**	**NSE**	**MRB**	**NVE**	**KGE**	**PFC**	**Model Improvement (%)**
Caniapiscau	0.80	0.02	0.75	0.83	0.31	0.83	0.00	0.79	0.88	0.30	7.77
La-Forge-1	0.85	-0.04	0.82	0.89	0.39	0.85	-0.01	0.82	0.90	0.42	-0.47
La-Grande-4	0.89	-0.06	0.86	0.89	0.46	0.91	-0.04	0.88	0.92	0.35	9.13
La-Grande-3	0.86	-0.06	0.84	0.86	0.44	0.87	-0.09	0.85	0.86	0.38	5.11
La-Grande-2	0.81	-0.08	0.77	0.84	0.45	0.81	-0.10	0.76	0.85	0.40	0.68
La-Grande-1	0.74	-0.07	0.70	0.73	0.46	0.78	-0.01	0.76	0.86	0.45	8.41
Eastmain-1	0.80	0.01	0.79	0.88	0.24	0.77	-0.01	0.75	0.87	0.27	-6.35
Lac-Opinaca	0.72	-0.02	0.71	0.83	0.31	0.72	-0.04	0.69	0.82	0.34	-1.17
Lac-Mesgouez	0.88	-0.10	0.83	0.88	0.31	0.83	-0.12	0.78	0.84	0.32	-16.21
Lac-Mistassini	0.85	-0.06	0.84	0.90	0.10	0.85	-0.09	0.83	0.87	0.01	-0.97

Sub-basin wise VALIDATION performance statistics for ANNUAL SAC-SMA models at LGRB

Sub-basin	*SAC-SMA DDM*					*SAC-SMA SNOW17*					Model Improvement (%)
	NSE	MRB	NVE	KGE	PFC	NSE	MRB	NVE	KGE	PFC	
Caniapiscau	0.89	0.02	0.87	0.89	0.25	0.88	0.00	0.86	0.94	0.24	-1.73
La-Forge-1	0.61	-0.06	0.57	0.72	0.44	0.59	-0.08	0.55	0.72	0.44	-2.87
La-Grande-4	0.71	0.06	0.69	0.80	0.48	0.75	0.04	0.74	0.87	0.33	8.10
La-Grande-3	0.53	-0.14	0.50	0.59	0.49	0.60	-0.12	0.58	0.65	0.47	8.19
La-Grande-2	0.68	-0.02	0.63	0.66	0.48	0.74	-0.05	0.70	0.72	0.46	9.30
La-Grande-1	0.75	0.02	0.65	0.75	0.46	0.80	0.05	0.74	0.79	0.48	10.14
Eastmain-1	0.79	-0.03	0.77	0.80	0.33	0.77	-0.07	0.74	0.83	0.34	-6.01
Lac-Opinaca	0.73	-0.14	0.69	0.63	0.36	0.75	-0.16	0.71	0.67	0.35	3.37
Lac-Mesgouez	0.58	-0.07	0.57	0.72	0.50	0.71	-0.09	0.68	0.81	0.44	17.62
Lac-Mistassini	0.31	-0.08	0.32	0.62	0.40	0.41	-0.06	0.41	0.69	0.36	7.08

Sub-basin wise VALIDATION performance statistics for SEASONAL SAC-SMA models at LGRB

	SAC-SMA DDM					SAC-SMA SNOW17					
Sub-basin	**NSE**	**MRB**	**NVE**	**KGE**	**PFC**	**NSE**	**MRB**	**NVE**	**KGE**	**PFC**	**Model Improvement (%)**
Caniapiscau	0.88	0.01	0.85	0.90	0.28	0.89	0.02	0.88	0.93	0.23	7.89
La-Forge-1	0.63	-0.04	0.59	0.74	0.45	0.65	-0.07	0.62	0.75	0.44	3.79
La-Grande-4	0.83	-0.02	0.78	0.83	0.49	0.73	0.00	0.72	0.84	0.53	-11.31
La-Grande-3	0.51	-0.20	0.48	0.56	0.50	0.56	-0.18	0.54	0.63	0.47	4.96
La-Grande-2	0.66	-0.19	0.60	0.58	0.49	0.70	-0.14	0.66	0.69	0.48	6.52
La-Grande-1	0.72	0.03	0.60	0.68	0.49	0.77	0.04	0.70	0.76	0.50	9.19
Eastmain-1	0.79	-0.01	0.77	0.81	0.32	0.79	-0.05	0.78	0.85	0.32	2.16
Lac-Opinaca	0.73	-0.13	0.70	0.64	0.36	0.70	-0.15	0.66	0.63	0.37	-5.96
Lac-Mesgouez	0.52	-0.14	0.51	0.69	0.52	0.48	-0.15	0.48	0.70	0.50	-4.09
Lac-Mistassini	0.29	-0.13	0.32	0.62	0.34	0.36	-0.09	0.38	0.68	0.42	5.10

Appendix D: Sub-basin wise model performance statistics at UASR

Sub-basin wise CALIBRATION performance statistics for ANNUAL models at UASR

Calibration performance

Sub-basin	MAC-HBV DDM					MAC-HBV SNOW-17					Model Improvement %
	NSE	MRB	NVE	KGE	PFC	NSE	MRB	NVE	KGE	PFC	
Kamsack	0.45	-0.09	0.41	0.63	0.54	0.12	-0.12	0.05	0.53	0.51	-26.22
Shellmouth Reservoir Inflow	0.48	0.03	0.47	0.74	0.47	0.51	-0.01	0.49	0.73	0.48	3.07
	SAC-SMA DDM					SAC-SMA SNOW-17					
Kamsack	0.63	0.14	0.55	0.76	0.38	0.70	0.01	0.60	0.83	0.34	9.79
Shellmouth Reservoir Inflow	0.70	0.06	0.64	0.82	0.43	0.67	0.10	0.63	0.80	0.38	-4.14

Sub-basin wise VALIDATION performance statistics for ANNUAL models at UASR

Validation performance

Sub-basin	MAC-HBV DDM					MAC-HBV SNOW-17					Model Improvement %
	NSE	MRB	NVE	KGE	PFC	NSE	MRB	NVE	KGE	PFC	
Kamsack	0.31	-0.29	0.23	0.27	0.58	0.02	-0.19	-0.20	0.23	0.67	-33.06
Shellmouth Reservoir Inflow	0.56	-0.14	0.50	0.57	0.53	0.19	-0.26	0.08	0.23	0.62	-39.17
	SAC-SMA DDM					SAC-SMA SNOW-17					
Kamsack	0.47	-0.11	0.36	0.53	0.57	0.30	-0.38	0.15	0.29	0.60	-14.72
Shellmouth Reservoir Inflow	0.49	-0.10	0.41	0.52	0.57	0.44	-0.15	0.27	0.49	0.60	-4.89

**Sub-basin wise CALIBRATION performance statistics for SEASONAL models at UASR**

Calibration performance

Sub-basin	MAC-HBV DDM					MAC-HBV SNOW-17					Model Improvement %
	NSE	MRB	NVE	KGE	PFC	NSE	MRB	NVE	KGE	PFC	
Kamsack	0.42	-0.08	0.28	0.52	0.53	0.57	-0.05	0.55	0.78	0.31	14.80
Shellmouth Reservoir Inflow	0.42	0.02	0.37	0.72	0.49	0.61	-0.03	0.58	0.78	0.45	17.67
	SAC-SMA DDM					SAC-SMA SNOW-17					
Kamsack	0.58	0.01	0.53	0.76	0.42	0.64	0.08	0.61	0.77	0.41	7.81
Shellmouth Reservoir Inflow	0.66	0.02	0.59	0.73	0.44	0.68	0.03	0.60	0.73	0.46	2.44

Sub-basin wise VALIDATION performance statistics for SEASONAL models at UASR

Validation performance

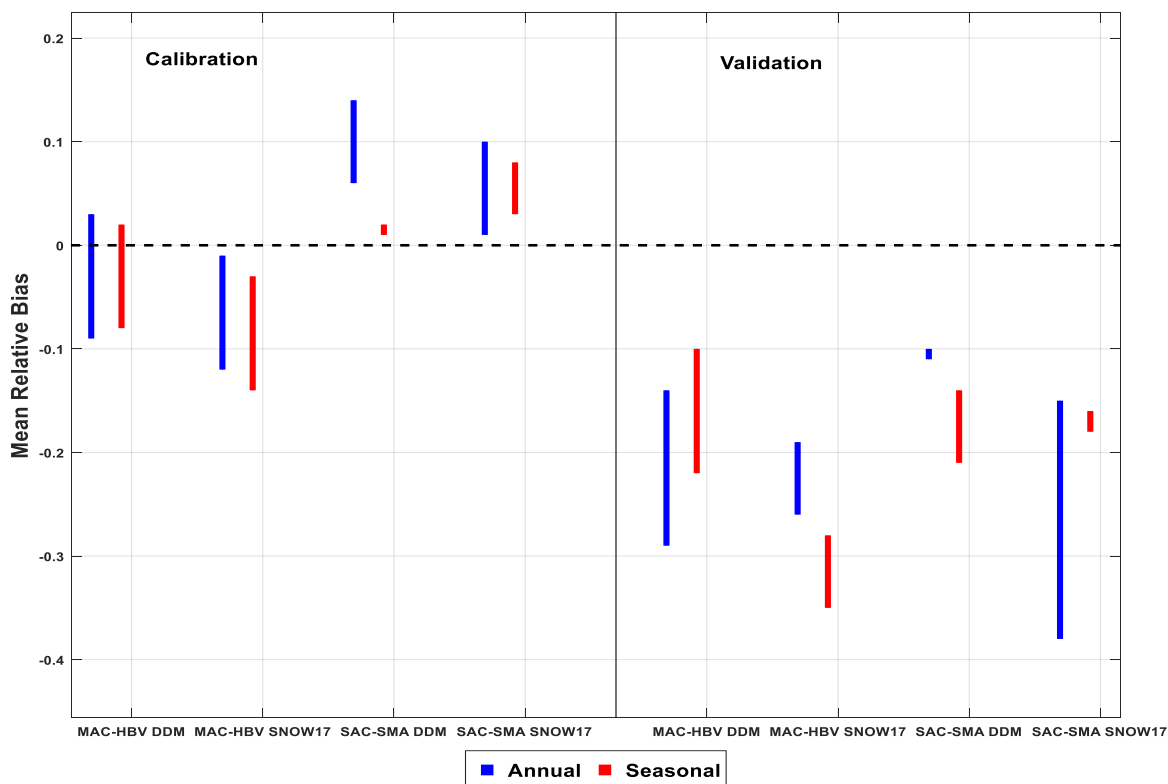| Sub-basin	MAC-HBV DDM					MAC-HBV SNOW-17					Model Improvement %
	NSE	MRB	NVE	KGE	PFC	NSE	MRB	NVE	KGE	PFC	
Kamsack	0.34	-0.22	0.24	0.26	0.59	0.19	-0.14	0.16	0.58	0.61	-10.93
Shellmouth Reservoir Inflow	0.52	-0.10	0.46	0.60	0.52	0.28	-0.28	0.23	0.35	0.61	-22.28
	SAC-SMA DDM					SAC-SMA SNOW-17					
Kamsack	0.58	-0.21	0.49	0.52	0.50	0.59	-0.18	0.40	0.52	0.51	1.87
Shellmouth Reservoir Inflow	0.58	-0.14	0.45	0.50	0.55	0.46	-0.18	0.32	0.48	0.59	-13.20

Appendix E: Model Performance Statistics - Mean Relative Bias (MRB)

Mean Relative Bias (MRB) statistics for MAC-DDM, MAC SNOW-17, SAC-DDM, SAC SNOW-17 model structures for annual and seasonal models of LGRB
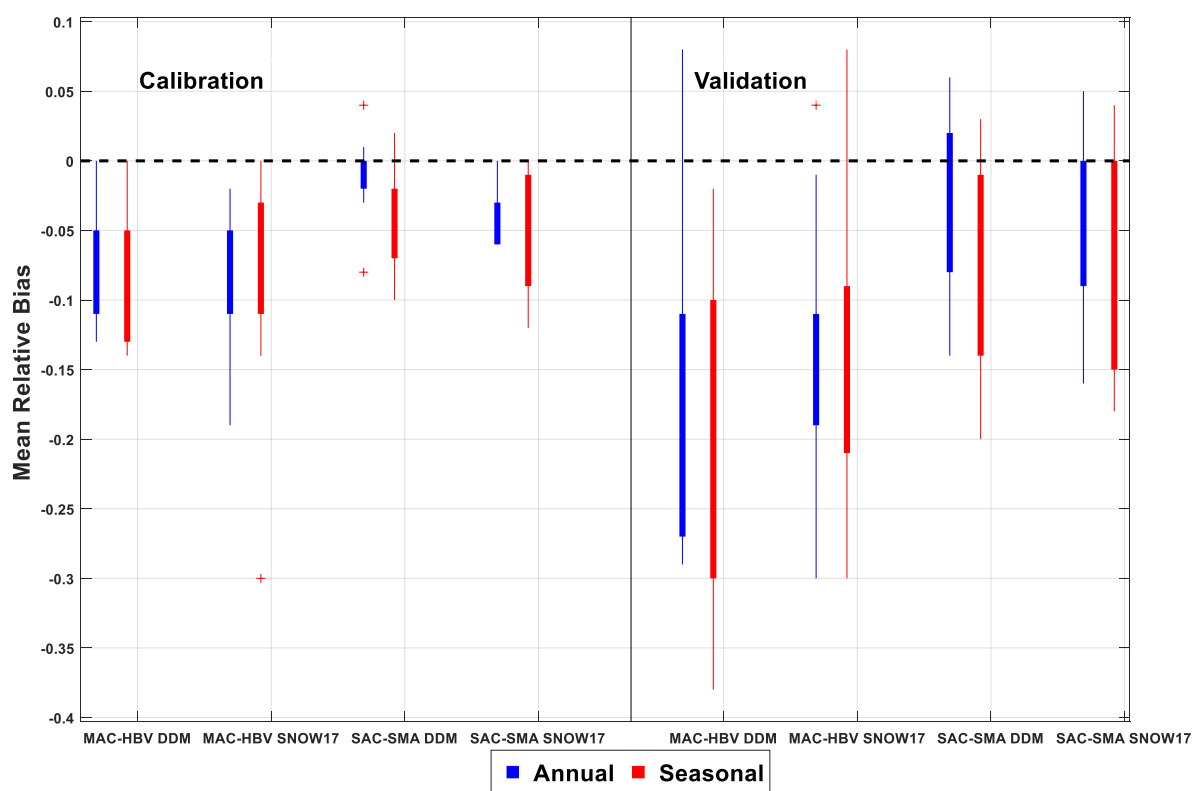
MRB is bound to zero (black dashed line) for perfect model and provides information on overall under-estimation (negative values) and overestimation (positive values) by model combinations.

Mean Relative Bias (MRB) statistics for MAC-DDM, MAC SNOW-17, SAC-DDM, SAC SNOW-17 model structures for annual and seasonal models of UASR

MRB is bound to zero (black dashed line) for perfect model and provides information on overall under-estimation (negative values) and overestimation (positive values) by model combinations.